Green Chemistry

Cutting-edge research for a greener sustainable future

www.rsc.org/greenchem

Volume 15 | Number 6 | June 2013 | Pages 1385–1696

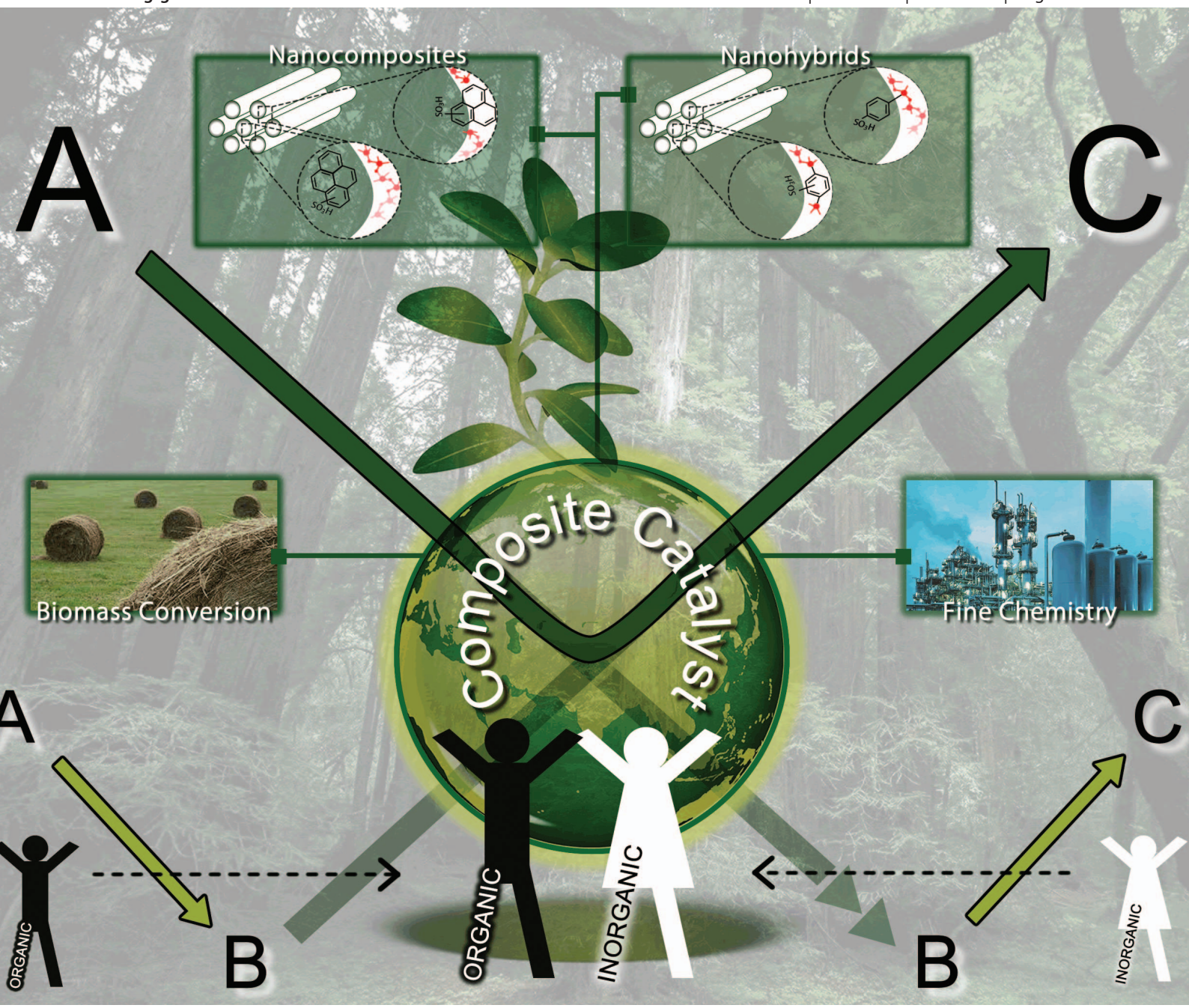

ISSN 1463-9262

RSC Publishing

TUTORIAL REVIEW

Bert F. Sels *et al.*

Tailoring nanohybrids and nanocomposites for catalytic applications

Green Chemistry

RSC Publishing

TUTORIAL REVIEW

View Article Online
View Journal | View Issue

Tailoring nanohybrids and nanocomposites for catalytic applications

Cite this: *Green Chem.*, 2013, **15**, 1398

Filip de Clippel,[a] Michiel Dusselier,[a] Stijn Van de Vyver,[a,b] Li Peng,[a,c] Pierre A. Jacobs[a] and Bert F. Sels*[a]

Received 31st December 2012,
Accepted 28th March 2013

DOI: 10.1039/c3gc37141g

www.rsc.org/greenchem

Research on and development of inorganic–organic nanohybrids and nanocomposite materials has attracted increasing attention in recent years. Synthetic strategies for such materials vary from grafting or co-condensation of Si and C sources to the impregnation of silica with polymers. Nanohybrids, prepared using organosilanes, and nanocomposites, obtained by hard or soft templated synthesis, are discussed. Various strategies will be presented that demonstrate how additional carbon properties can be exploited maximising the activity, selectivity and stability of composite materials as solid catalysts. Composite materials allow for the extensive engineering of a catalyst enabling careful tuning of the type, amount and position of active sites, as well as the porosity and hydrophilic nature of the final catalyst. These materials not only combine the advantages of silica (*e.g.* thermal stability, rigidity, ordering) and carbon (*e.g.* flexibility, ductility) but also allow their synergetic action in various catalytic applications.

1. Introduction

Innovative composite materials offer an exciting opportunity to address current challenges in catalysis and green chemistry. A reduction of the constituent dimensions of the composite down to the molecular scale makes it possible to control and fine-tune the ultimate material properties.[1] The engineering of such materials, which are obtained *via* direct synthesis

[a]*Centre for Surface Chemistry and Catalysis, KU Leuven, Kasteelpark Arenberg 23, 3001 Heverlee, Belgium. E-mail: bert.sels@biw.kuleuven.be; Fax: +32 16 321998; Tel: +32 16 321610*
[b]*Department of Chemical Engineering, Massachusetts Institute of Technology, Cambridge, MA 02139, USA*
[c]*Instituto de Tecnología Química, UPV-CSIC, Valencia 46022, Spain*

Filip de Clippel

Filip de Clippel obtained his masters degree in bio-engineering (catalytic technology) at KU Leuven in 2006. He spent a prolonged period at the University of Seville in Spain and examined the confined growth of carbon nanotubes in zeolites under the supervision of Prof. P. A. Jacobs for his master thesis. In 2012 he finished his PhD on the use of silica–carbon nanocomposites for adsorption and catalytic applications under the supervision of Prof. Sels and Prof. Jacobs. His post-doctoral research focusses on the development of tunable multifunctional and porous carbon and composite materials and their use in catalysis (photocatalysis and biomass conversion) and gas separation.

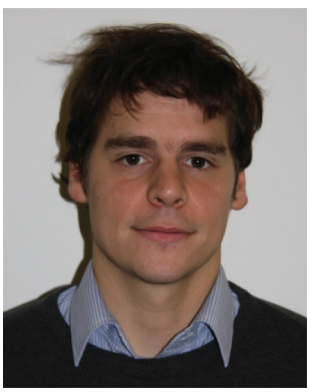

Michiel Dusselier

Michiel Dusselier obtained a Master of engineering in Catalytic Technology at KU Leuven in 2009. He performed a part of these studies at the Technische Universität München, Germany. His master thesis was performed under the guidance of Prof. Sels and Prof. P. A. Jacobs and dealt with the conversion of cellulose with heterogeneous catalysts. Now he is in the process of finishing his PhD under the guidance of Prof. Sels, dealing with the tailoring of catalytic routes towards and from lactic acid, as well as examining novel renewable monomers and their polymers.

methodologies or organic post-modification approaches, opens up new prospects for catalytic applications.

Among the composite materials, nanohybrids and nanocomposites should be unambiguously defined, to avoid the inconsistencies in the scientific literature. For the present purpose, a nanocomposite is defined as a material in which one of the components is within the size range of 1–100 nm. More specifically, the nanocomposite comprises two components of which one is a predefined entity such as a nanocluster or a nanoblock. The term 'nanohybrid' is used when the inorganic units of the hybrid are formed *in situ* from individual building blocks or when a covalent bond exists between the two different units.[2]

Several excellent reviews have been published on the synthesis and properties of inorganic–organic nanohybrid[3] and nanocomposite materials.[4] Besides highlighting the most recent progress in the synthesis approach, the present review also mainly focuses on a discussion of the usage of composite materials for catalytic purposes with an emphasis on fine chemicals synthesis and biomass conversion. Porous carbon materials are mainly discussed as reference materials. For a more detailed discussion on (ordered) porous carbons and their use in catalysis, we would like to refer the reader to its dedicated scientific literature.[4–8]

Ordered mesoporous silica (OMS) is often at the centre of catalytically active composite design because of a combination of interesting properties such as a high surface area with a robust yet flexible (*e.g.* in pore size and functionalisation) structure. Moreover, the pore arrangements make them ideal objects for characterisation studies, while the pore architecture is usually highly accessible to most common reagents.[9] Such properties are essential for tuning and transforming the composite into a highly performing catalyst.

The initially reported design of nanohybrid catalysts comprised the simple attachment of organic groups such as carboxylic acids, sulphonates or amines, which act either as the catalyst or function as docking sites for catalytically active metals, organometallic complexes, enzymes, *etc.*[3f] The potential of this type of composite is not limited to the introduction of an active site. More evolved nanohybrid design could recently demonstrate additional modifications of other chemical and physical properties like polarity, texture, porosity and structural rigidity. Such modifications significantly expand flexibility in catalyst development. Several examples of modifications and their impact on the catalytic performance will be given. The option of introducing multiple active sites is a unique opportunity to engineer catalysts for their application in multistep or cascade reactions, as is often required in biomass valorisation. Independent incorporation of different active sites and precise control of their positioning are crucial parameters inducing and optimising unique cooperative actions.

The second material type, *viz.* the nanocomposite catalyst, usually contains a silica matrix with a non-bonded (hydro) carbon component. Similarly, several modification tools are available to change the chemical and physical properties of the composite to improve its catalytic performance.

The present review is organised in two parts. First, it concentrates on the different synthetic strategies for preparing OMS-based nanohybrids and nanocomposites. A distinction between both groups was made based on the location of the organic matter (Scheme 1). The carbon phase is either occluded in the pore voids of the parent OMS or resides in/on the pore wall along with the silica. Secondly, an extensive discussion is presented on the use of composite materials in catalysis. The versatility of the physico-chemical properties and

Stijn Van de Vyver

Stijn Van de Vyver obtained his BSc and MSc degrees from KU Leuven (Belgium). In 2012 he graduated with a PhD in Bioscience Engineering under the supervision of Prof. Bert Sels and Prof. Pierre Jacobs. His thesis work involved the catalytic conversion of cellulosic biomass into platform molecules used for the production of biofuels and industrially important chemicals. He was awarded a fellowship from the Belgian American Educational Foundation and an honorary Fulbright grant to do postdoctoral research at the Massachusetts Institute of Technology, where he is currently working in the group of Prof. Yuriy Román.

Li Peng

Li Peng obtained her PhD (2005) from Jilin University, China, under the guidance of Prof. Ruren Xu and Prof. Jihong Yu to work on the synthesis and intercalation chemistry of layered aluminophosphates. After a short term postdoctoral research in Korea Advanced Institute of Science and Technology (KAIST), Korea, she joined the research group of Prof. Sels and Prof. P. A. Jacobs as a postdoctoral fellow at KU Leuven in 2007 and dealt with the synthesis of mesoporous carbon and carbon/silica hybrid materials as well as their catalysis application until 2011. Now she is a scientific researcher in the Instituto de Tecnología Química UPV-CSIC, Spain, and her research deals with the design and synthesis of novel zeolites and related inorganic open framework materials.

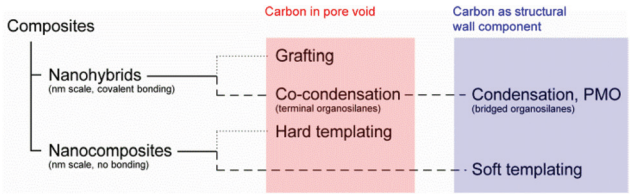

Scheme 1 Classification of the composites discussed. The dotted and dashed lines represent direct synthesis and post-synthetic modification methodologies, respectively. PMO: periodic mesoporous organosilica.

their modifications are discussed with an emphasis on the relationship of the properties with the catalytic performance. Whereas the former is done in terms of active site (density), pore size, surface area, polarity, multi-functionality and compartmentalisation, the latter is based on catalytic selectivity, activity and stability. To improve the readability of this review a list of frequently used abbreviations has been provided in Table 1.

2. Synthesis of nanohybrids and nanocomposites

Nanohybrid and nanocomposite materials are both obtained by direct synthesis routes or post-synthetic modification strategies. Most of the latter procedures use OMS as the inorganic structural matrix. The direct synthesis methods usually apply adapted OMS synthesis procedures using an additional carbon source like organosilanes, resins and carbohydrates. Although the use of OMS or the ultimate formation of well-ordered mesoscopic phases is not always a prerequisite for their catalytic potential, they show the following properties: (i) well-ordered mesoporous structures for an unambiguous structural investigation and sufficient reagent accessibility, (ii) a large surface area for high catalytic activity, (iii) sufficiently high rigidity and thermal stability for catalytic use under relevant conditions, and (iv) ease of surface modification and flexible synthesis procedures in terms of building blocks and pore size variation for a wide range of catalyst design and development.

The impressive variety of parent OMS includes materials denoted as M41S, SBA, HMS, KIT-1, MSU-1, TUD-1, HMM-33, FSM-16, and COK-12 (Table 2). It should be stressed that strictly speaking, not all of them exhibit a mesoscopic ordering of their pore structure. While hexagonal and cubic ordering has been reported for the M41S family, SBA types, and COK-12, others such as KIT-1, TUD-1, MSU-1, HMM-33, and HMS show a rather disordered pore arrangement. Various morphologies are reported to exist within the OMS group: worm-like to spherical for MCM-41, nanoplates for COK-12 and SBA-15, and irregular forms for MCM-48, KIT-1, TUD-1 and MSU-1 (Table 2). Irrespective of the particle shape, the pore orientation with respect to the external surface is crucial to ensure adequate reagent accessibility of the interior during the composite synthesis and efficient reactant diffusion during a catalytic reaction with the composite. It is generally accepted that worm-like materials are inferior in this respect, while the recently developed thin platelets of SBA-15[10] and COK-12[11] with perpendicularly oriented mesopores provide highly accessible OMS materials. Spherical morphologies show good accessibility as well.

Next to morphology, appropriate accessibility is ascertained preferably when either intersecting pore channels like in SBA-1, SBA-15 and MCM-48, or uniform pore sizes like in the disordered silicas, denoted as TUD-1, KIT-1 and MSU-1 are

Pierre A. Jacobs

Pierre A. Jacobs is, since 2008, professor emeritus with special mandate at KU Leuven. One of his present responsibilities concerns the implementation of advanced safety procedures in chemical labs. During his active career, he has been Professor of Physical-Chemistry and Catalysis at KU Leuven and authored over 600 reviewed papers. The industrial impact of his research is visible in his numerous patents. Among the important awards he received for his research can be mentioned: the Paul Emmett Award in 1981 for his contribution to fundamental understanding of zeolite catalysts, the Donald Breck Award in 1998 for his work on zeolite-based biomimetic catalysis. In recognition of his contributions to bridging homogeneous, heterogeneous and bio-catalysis, he received the Synetix Award and the Kreitman Award in 2001.

Bert F. Sels

Bert F. Sels obtained his PhD in 2000 at KU Leuven on oxidation chemistry, after which he did a post-doc with BASF until 2002. Another 3 years post-doc for the National Science Foundation was dedicated to the 'activation of nitrous oxide' and the 'microscopic imaging of catalytic events in single particles'. He became Assistant Professor in 2003, teaching courses on analytical organic chemistry, sustainability and heterogeneous catalysis. He has been Full Professor since 2006 in the Faculty of Bioscience Engineering, Leuven. He has published about 160 scientific papers and 11 patents, and is the recipient of numerous awards including the international DSM chemistry award. His current research explores heterogeneous catalysis for converting renewables such as ligno(hemi)cellulose and small molecule activation.

Table 1 List of abbreviations

OMS	Ordered mesoporous silica	EAS	Electrophilic aromatic substitution	(P)FA	(Poly)furfuryl alcohol
PMO	Periodic mesoporous organosilicas	OMC	Ordered mesoporous carbons	AMS	α-Methyl styrene
TEOS	Tetraethoxysilane	PF	Phenol-formaldehyde	FC	Friedel–Crafts
TMS	Trimethoxysil(yl)(ane)	EISA	Evaporation induced self-assembly	*p*TSA	*p*-Toluene sulphonic acid
TES	Triethoxysil(yl)(ane)	RF	Resorcinol-formaldehyde	CSPTMS	2-(4-Chlorosulphonylphenyl)-ethyltrimethoxysilane
MPTMS	Mercaptopropyl trimethoxysilane	PSS	Polymer/silica/surfactant	HMF	Hydroxymethyl furfural
BSFTA	Bis(tri-methylsilyl)-trifluoroacetamide	PEO-*b*-PS	Poly(ethylene oxide)-*b*-polystyrene	BPA	Bisphenol A
APT(M/E)S	Aminopropyl tri(m)-ethoxysilane	CMS	Carbogenic molecular sieves	TEMPO	2,2,6,6-Tetramethyl-1-piperidinyloxy
ATRP	Atom transfer radical polymerisation	(M/D/T)MA	Mono-/di-/tri-methylamine	TFHTFMESS	1,2,2-Trifluoro-2-hydroxy-1-tri-fluoromethyl-ethane sulphonic acid β-sultone

Table 2 Overview of selected mesoporous silica and their physical properties

	Ordering	Morphology	Wall thickness[a]	Pore diameter[a]	Ref.
SBA-15	Hexagonal	Fibers	3.1–6.4	4.6–30.0	13*a*
	Hexagonal	Prism, sphere, donut, rod, rice shape	3.0–4.6	6.3–8.9	16
	Hexagonal	Platelets	3.0–5.1	6.5–22.0	10
COK-12	Hexagonal	Platelets	4.2–4.4	5.5–6.0	11
FSM-16	Hexagonal	Flakes	1.5–1.8	2.2–2.8	17
MCM-41	Hexagonal	Prism	—	1.6–10.0	9 and 18
	Hexagonal	Curved rod	1.5–1.7	2.7–3.3	19
	Hexagonal-cubic	Sphere	1.0–1.6	2.4–3.3	19*b* and 20
SBA-1	Cubic (*Pm3n*)	(Truncated) cube, sphere, octahedron	—	2.0–3.2	12*a* and 21
MCM-48	Cubic (*Ia3d*)	Irregular, sphere	~1.0	1.9–4.1	18 and 22
KIT-1	Disordered	Irregular	—	3.4	23
MSU-1	Disordered	Irregular	—	2.0–5.8	24
TUD-1	Disordered	Irregular	2.5–4.0	2.5–25	25
HMS	Disordered	Sphere	1.0–1.6	2.1–4.5	26
HMM	Disordered	Sphere	—	4.0–15.0	27

[a] Expressed in nm.—: no information available.

available. Two types of pore interconnectivity can be distinguished in OMS. Meso-/mesopore connection appears in disordered silica and MCM-48, while micro-/mesopore connection occurs in the structure of SBA-15. In addition, mesoporous cage-like pores interconnected with smaller pores exist in ordered silicas such as SBA-2[12] or -16,[13] KIT-5[14] and FDU-1.[15] Such interconnections could prove beneficial in catalysis by reducing mass transfer restrictions and pore blocking.

Structural integrity, on the other hand, is an issue during the synthesis of the composite material, while the (hydro) thermal stability is crucial during catalysis. Sufficient thickness of the pore wall often is a prerequisite for the mechanical stability of the materials, while hydrophobicity determines the hydrothermal stability of OMS. Members of the SBA family, TUD-1 and COK-12 materials, show thicker pore walls ranging from 4 to 6 nm. FSM-16, MCM-41, MCM-48 and HMS have wall thickness between 1 and 2 nm.

Several of the OMS members are useful in the design of composite materials. As defined in the Introduction, the composite materials were classified into two families depending on the specific interactions between the organic and inorganic components, *viz.* nanohybrids and nanocomposites (Scheme 1). The nanohybrids cover materials containing an organic phase at the molecular level covalently attached to the OMS surface, encompassing subfamilies of materials prepared either *via* grafting or direct synthesis. A variety of organosilanes has been used as organic building blocks in both synthesis strategies. Grafting and direct co-condensation make use of terminal organosilanes, while bridged organosilanes are condensed to obtain the so-called periodic mesoporous organosilicas (PMOs). Nanocomposites, at the nano-meter scale showing distinct non-bonded silica and carbon domains, are obtained either by pore filling *via* conventional impregnation of a parent OMS with organic compounds, or *via* alternative OMS synthesis recipes involving the use of an additional (hydro) carbon source. Both procedures are known as hard and soft templating synthesis procedures, respectively. The latter nanocomposite material thus contains mesopores with entangling silica and carbon phases in the pore walls.

2.1. Silica–carbon nanohybrids

Two major synthesis strategies are reported to obtain a silica–carbon nanohybrid: (i) grafting of a predefined OMS with silane agents, or (ii) co-condensation of both inorganic and

organic building blocks, *viz.* tetra-alkoxysilanes (*e.g.* tetraethoxysilane, TEOS) with trialkoxyorganosilanes or bis-silylated organic units, respectively, in the presence of a structure-directing agent. The functional group of the organic component serves as a catalyst, as an anchoring site for catalytically active sites or as a means to tune the surface polarity and the pore size of the nanohybrid.

2.1.1. Grafting. Grafting is often the preferred synthesis tool because of its versatility and ease of handling. Modification of the silica surface involves reaction of a surface silanol group with a silane coupling reagent, preferably being a terminal organosilane (Fig. 1, left). The chemical structure of the organosilane comprises a Si atom covalently bound through a Si–C with a (functionalised) hydrocarbon and attached to at least one alkoxy-, halo-, acyloxy- or amino leaving group. A wide range of organosilanes has been applied as a grafting agent in the context of catalysis (Table 3). Catalytically active functional groups introduced in OMS using the grafting synthesis technique are, among others, thiols, cyanides, amines, carboxylic acids and sulphonates. The chemical functionality either forms the active site, sometimes after a preceding transformation of an active site precursor, or the anchoring site enabling to attach more complex catalytic centres such as enzymes and organometallic complexes to OMS.

The efficiency of the grafting methodology is determined by the number of reactive surface silanol groups on the OMS, the accessibility of the OMS silanols for the grafting agent, the reactivity of the grafting agent, and the efficiency of the precursor transformation into a catalytic active site. Due to the nature of the silylation (grafting) reaction, the presence of sufficient silanol groups on the silica surface is required. OMS have a high surface area with a silanol density of 1–3 silanols per nm^2.[22b,28] Although this amount is somewhat lower than on conventionally precipitated amorphous silica (4–6 silanols per nm^2),[28b,29] it is sufficiently high to decorate the OMS surface with an abundant number of organic functional groups. MCM-41 with a surface of 800 $m^2\ g^{-1}$ and 1 silanol group for every 3 Si atoms holds about 4 silanols per nm^2,[30] which approaches the theoretical maximum silanol density on silica.[31] An additional hydrothermal treatment of the silica was suggested as resulting in an increase of the amount of silanols. Accordingly, nanohybrids have been reported with a significant increase of the functional group density. After additional refluxing of calcined MCM-41 in water for 3 h prior to grafting, an increase of the organic functional groups from 0.7 to 1.7 mmol g^{-1} has been reported.[32] Alternatively, if an extraction method replaces calcination as a procedure to remove surfactant molecules, the thermal elimination of silanol groups is significantly suppressed. In this way, upon grafting MCM-41 and MCM-48 with mercaptopropyl-trimethoxysilane (MPTMS), the sulphur loading could be increased from 3.5 to 7.8 wt% and from 4.8 to 15.6 wt%, respectively.[33]

Whereas the content of grafted organic species can further be controlled by changing the concentration of the organosilane in the grafting solution,[33] its maximum yield is obtained when an excess of the silylation agent is used. However, the ultimate amount of grafted organic moieties present is generally lower than that expected based on the silanol content, with typical variations between 0.5 and 1.5 mmol g^{-1} depending on the nature of the silylation agent and OMS.[34]

Grafting efficiency is another important concern. Ideally, the silylation agent is volatile, allowing ready removal of excess agent. Furthermore, the reactivity of the silylation agent is determined by its leaving group. Reactive silanes mostly contain halide, acyloxy or amino leaving groups, the less reactive alkoxy and allylsilanes requiring a silylation procedure at elevated temperature. Potential side reactions of the leaving

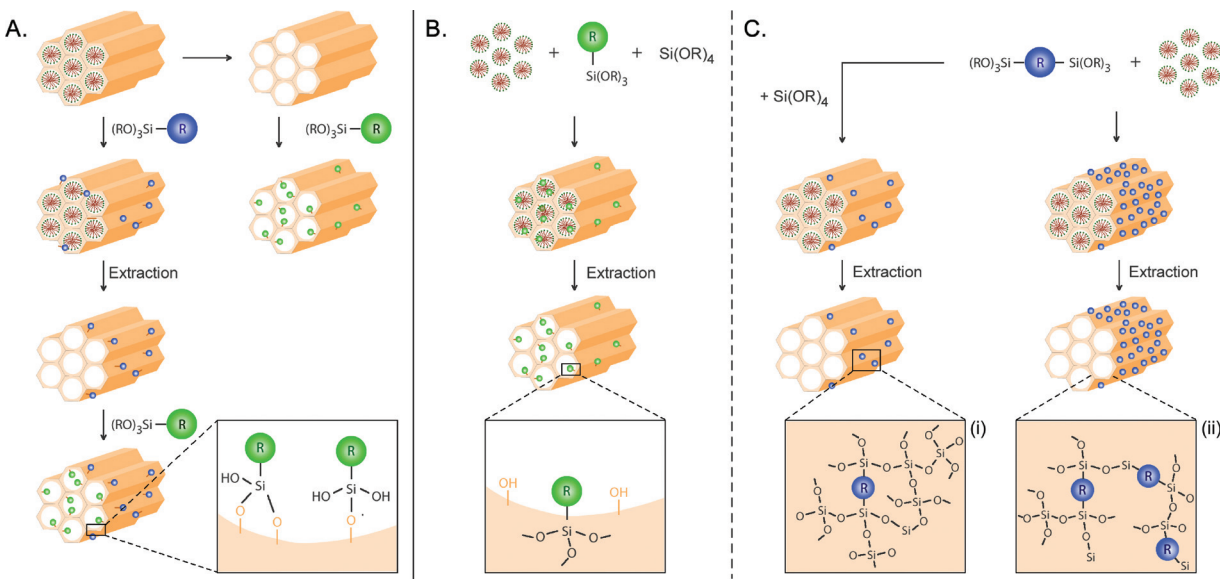

Fig. 1 Schematic presentation of various silica–carbon nanohybrid synthesis routes by organosilane modification of ordered mesoporous silica: grafting (A), co-condensation with terminal organosilanes (B) and (i) co-condensation or (ii) condensation with bis-silylated organic units (C).

Table 3 Overview of a selection of recently reported organosilicas as obtained by grafting or (co-)condensation

Methodology	Agent[a]	Functionality[b]	Reference
Post-synthesis			
Grafting	3-Triethoxysilylpropylisocyanate	Salen complex (anchoring)	39
	3-Mercaptopropyl TMS	Salen complex, pyridine (anchoring)/ sulphonic acid (oxidation)	40, 41/28 and 38
	3-(ChloroDMS)-propyl bromo-isobutyrate	Sulphonic acid (ATRP)[c]	42
	3-Aminopropyl TMS	Amine/enzyme (anchoring)	43/44
	3-Aminopropyl TES	Sn/Pd/Zr/Ni/In Complex, Keggin complex (anchoring)	45 and 46
	3-(TES)propyltriphenyl phosponium bromide	Phosponium bromide	47
	N-Methyl-*N*-(TMS) trifluoroacetamide	/	48
	Triethoxyfluorosilane	/	49
Direct synthesis			
Co-condensation	3-Mercaptopropyl TMS	Sulphonic acid (oxidation)	32 and 50
Terminal organosilane	Phenyl TES	Sulphonic acid (sulphonation)	50
	Methyl TMS	/	50
	2-(4-Chlorosulphonylphenyl)-ethyl TMS	Sulphonic acid (hydrolysis)	51
	Benzyl methyl-(3-TMS-propyl)-amine// 2-(4-chlorosulphonylphenyl)ethyl TMS	Amine//sulphonic acid (hydrolysis)	52
(Co-)condensation	1,4-Bis(triethoxysilyl)benzene	Sulphonic acid (sulphonation)	53 and 54
Bridging organosilane	Bis[3-(triethoxysilyl)propyl]disulphide	Sulphonic acid (oxidation)	55
	Bis(triethoxysilyl)ethylene	Sulphonic acid (Diels–Alder/sulphonation)	56
	1,2-Bis(trimethoxysilyl)ethane	Perfluoroalkyl sulphonic acid (grafting)	57
	Bis(trimethoxysilyl)trityl cation	Triphenylmethylium cation	58

[a] TMS = trimethoxysil(yl)(ane), TES = triethoxysil(yl)(ane). [b] Strategy applied for the acquirement of the specified functionality denoted in parentheses. [c] Atom transfer radical polymerisation (ATRP).

groups with the hydroxylated surface are to be avoided. As an example, alkoxy and halide leaving groups are able to form alcohols and alkylammonium halides which are hard to remove.[35] In addition, halides induce leaching of isomorphically substituted heteroatoms from the silica network.[36] In this regard, a wide range of trimethylsilylation agents has been evaluated, such as trimethylsilylchloride,[37,38] hexamethyldisiloxane,[37,38] bis(tri-methylsilyl)trifluoroacetamide (BSFTA)[36] and hexamethyldisilazane.[35] The silazane silylation agent reacts in less severe conditions and allows a slow monofunctional surface reaction to occur, while the ammonia by-product is easily removed by thermal desorption.[35] Surface reaction with highly reactive BSTFA happens under even milder conditions, although sterical hindered silanols are not modified by this bulky agent.[36]

Recently, less moisture-sensitive alternatives such as aryl,[28b] allyl,[59] and methallyl[60] organosilanes have been suggested to improve the grafting efficiency. Such organosilanes benefit from an easy chromatographic purification after synthesis. They can be handled under hydrolytic conditions, resulting in a simplified grafting procedure. Indeed, high grafting efficiencies have been reported even under conditions where water was not completely removed.[28b,59,60] If the more reactive methallylsilane is used, the silylation can even be performed at room temperature.[60]

Moreover, the grafting efficiency also suffers from mass transfer limitations or from low adsorption of the silylation agent in the pores of OMS due to a mismatch in size and polarity, respectively. Next to this match between OMS pores size and the silylation agent size, also the presence of mesopore/mesopore interconnectivity can be beneficial. Diffusion limitations have been encountered with relatively large organosilanes, especially in small pore OMS, devoid of intersecting channels, *viz.* MCM-41. Consequently, grafting of MCM-41 often yields functional groups that are concentrated at the outer surface and pore mouths of the silica.[61] Likewise, a mismatch in polarity between the OMS surface and the silylation agents will severely limit pore diffusion of the organosilanes, preventing homogeneous chemical deposition of the organic moiety inside the silica pores.

Finally, if the synthesis of the nanohybrids relies on the introduction of an active site precursor, the efficiency of the additional chemical or thermal transformation is superimposed on the initial grafting efficiency. For instance, sulphonic acid groups are usually obtained after oxidation of grafted thiols using H_2O_2. The oxidation is generally incomplete, especially at high sulphur loadings because of the formation of inactive disulphide species during oxidation.[32,33,62]

Control over the precise location of the grafted functional groups is another key topic, especially when multifunctionality and optionally compartmentalisation is of concern. Multifunctionality has been obtained by mixing compatible silylation agents in one pot, resulting in a random distribution of the organic functions on the silica surface. A more precise control of the position of multiple functions is accomplished by performing two consecutive grafting procedures, one before and one after the removal of the structure directing surfactant molecules. As such, OMS are modified with two distinct organic groups, which are located inside the silica pores and on the external surface, respectively (Fig. 1A). In addition, the introduction of multiple functional groups in OMS has been demonstrated by grafting with complex organosilanes carrying

both thiol and amine protecting groups and subsequent thermolysis.[63] Neighbouring amine and thiol functional groups were created at the silica surface.

Grafting is also accompanied by a change in pore volume and pore size depending on the molecular size of the silylation agent. It is of utmost importance to account for this parameter with regard to catalytic applications. Irrespective of the intrinsic catalytic properties of the active site in the pore, mass diffusion limitations can limit both the actual activity and selectivity of the catalytic process. Grafting also affects the polarity of the nanohybrid structure due to a decrease of the number of free surface silanol groups and is related with the chemical structure of the organic moiety. The polarity of various organo-modified silicas and their hydrophobicity were reported to increase according to the nature of the organic group in the following order: cyanoethyl < aminopropyl < imidazole < benzyl < chloropropyl < trimethyl-silyl.[64] This order corresponds well with the polarity values of the corresponding liquids.[64] Obviously, polarity of the grafted solid can also be tuned by the amount of grafted species.

In conclusion, by applying the grafting procedure, a limited control of the amount, the physico-chemical properties (in terms of functionality, hydrophilicity balance, *etc.*) and the positioning of the organic groups can be obtained.

2.1.2. (Co-)condensation. Co-condensation is a direct synthesis method comprising the condensation of tetra-alkoxysilanes as the main Si-source with end-group (terminal) organosilanes as the C-source under acid, basic or nucleophilic conditions. Addition of a surfactant to the synthesis gel has been reported to yield an ordered mesoporous hybrid organosilica material with covalently linked phenyl, *n*-octyl, 3-aminopropyl and 2-cyanoethyl groups (Fig. 1, middle).[65] In general, this method results in a more uniform distribution and a higher loading of the functional groups compared to the grafting procedure.[55,58] Loadings up to 3 mmol g^{-1} of organic moieties seem possible *via* condensation with 3-aminopropyltrimethoxysilane (APTMS).[66] Positioning of an increasing number of pendent groups in the pore voids of the organosilica results in a reduction of the unit cell dimensions and the pore size (section 3.1). Pore ordering often deteriorates due to the disturbed interaction between the different Si sources and the structure directing surfactant. The use of mixed surfactants has been suggested to improve the packing of the surfactants as the short chain surfactants compensate the space occupied by the pending organic moieties of the organosilanes.[67] The use of alternative short-chain alkylamines in addition to alkylthiol functionalities beneficially influences the pore size and surface area.[50]

The type of organosilane regulates the final organic functionalities inside the silica pores, while the tetra-alkoxysilanes are at the origin of the surface silanol groups. Polarity studies using Reichardt's dye demonstrated that, for organic contents up to 1.1 mmol g^{-1}, the nanohybrids show a limited decrease in hydrophilicity compared to pure porous siliceous materials. The use of propylamine pendent groups results in a hydrophilicity decrease as the value of E_T^N, indicative of hydrophilicity and measured by the absorbed energy for the π–π* transition of the adsorbed dye molecules,[64] drops by 9%. This observation contrasts with the steep reduction of hydrophilicity after grafting: propylamine grafting results in a 42% decrease of the E_T^N value.[66] Such polarity differences for the same functionality are interesting when a basic catalyst is required in either a polar or apolar environment. Tuning of the final material properties of the porous co-condensate nanohybrid is achieved by controlling the ratio of the two silica precursors in the reaction mixture. If a further transformation of the functional group into a catalytic active site is required, the efficiency of this transformation is crucial for the catalytic performance. Similar to grafting (section 2.1.1), the conversion of thiol functions can be accomplished by a post-synthetic oxidation with HNO_3[68] or H_2O_2.[69] The post-treatment slightly decreases the mesoscopic ordering, while the oxidation is incomplete.[61c,68b,69] The oxidation degree brought to completion by prolonging the duration of the oxidation is not possible without further deterioration of the ordering.[69] Pore size and surface area after such treatment are significantly reduced.[62,68a,69] Alternatively, H_2O_2 can be added to the synthesis gel.[69,70] The efficiency of the thiol to sulphonate conversion is essentially complete with an appropriate amount of oxidant even at high thiol loadings. The observed coincident increase of the mesoscopic ordering was explained by the alteration of solvent and hydrophilic–hydrophobic interphase conditions, promoting the nanophase separation of the triblock copolymer template.[69]

Next to terminal organosilane building blocks, organosilica gels were synthesized by condensating bis-silylated organic agents, also referred to as silsesquioxanes or bridging silanes.[71] With the appropriate surfactant in the synthesis gel, ultimately PMOs could be obtained (Fig. 1C). Pioneering work on bridged organosilanes is available.[72,73] As the organic groups belong to the nanohybrid silica wall, they represent a structural component imparting unique chemical and physical properties to the material. The use of ethylene or phenylene bridged organosilanes yields amorphous or crystalline organosilica pore walls, respectively. The latter provides an additional robustness that can be exploited in catalysis (*vide infra*).[74] If only bridged organosilanes undergo condensation, a nanohybrid material with periodically alternating organic and silica surroundings is obtained. So far only a limited amount of organic moieties has been successfully incorporated into a PMO framework, *viz.* ethane,[72,75] ethylene,[73,75] benzene,[76] biphenylene and thiophene.[76a] Alkyl bridging units generally decrease the pore ordering and nanohybrid porosity, while incorporation of aromatic functionalities provides highly ordered and porous PMO.

Next to the bridge type, the stability of the C–Si bond is one of the main parameters to achieve high pore ordering in the hybrid material, obviously because the organic component is part of the structural framework. The importance of the silsesquioxane type has been demonstrated by the incorporation of ethylene bridged organosilanes which, at slightly elevated temperatures (*i.e.* 300 °C), are able to react with surface

silanols or with atmospheric oxygen. The bridging groups were transformed into terminal vinyl groups before being released as gaseous ethene and ethane. At 900 °C all organic groups were removed and a mesoporous silica was obtained with reduced unit cell size.[77] The synthesis of PMOs has been reported with (i) non-ionic, non-toxic, biodegradable and cheap alkylethylene oxide surfactants such as P123 and Brij-56/76 in acidic media[51,78] and (ii) cationic surfactants like CTAB in alkaline media.[72,75,76b,79] The harsh hydrolysis conditions can become problematic. Although ethylene, methylene and ethane in acidic media represent stable bridging organosilanes, more complex bridging organic precursors such as bridging benzene and thiophene proved instable. Cleavage of the Si–C bond is prevented by aging at room temperature or decreasing the acid concentration, as ascertained by solid state ^{29}Si NMR,[76a] but not without lowering the structural ordering. A decreased hydrolysis of the siloxane source during synthesis in a less acidified medium causes a reduced interaction of the ionic surfactant with the silicate species. Accordingly, a drop in degree of polymerisation and thus synthesis yield has been observed. In an alternative PMO synthesis route, the silicate source with cetylpyridinium chloride is mixed in an aqueous solution with a subsequent neutralisation step with $NaHCO_3$. After the addition of NH_4F and aging, ordered nanohybrids with stable Si–C bonds have been reported.[76a] Despite the careful adjustment of synthesis conditions, attempts using acetylene or bulkier bis-thiophene silsesquioxanes[76a] keep suffering from a highly instable Si–C bond or from disordered structures, demonstrating the importance of selecting a proper silsesquioxane precursor.

Various research groups demonstrated the successful synthesis of a highly ordered PMO with conservation of high surface area and porosity following a microwave-assisted synthesis procedure. Synthesis times were significantly reduced and a strict and better control of the synthesis was claimed.[80]

PMOs typically require an additional step in the synthesis procedure to introduce functional groups of use in catalysis. First a highly reactive yet catalytically inactive organic moiety is incorporated into the nanohybrid pore wall, followed by an activation treatment (Fig. 6). Aromatic moieties like benzyl groups have been activated by electrophilic aromatic substitution (EAS) such as nitration,[74] sulphonation,[50,76b] alkylation, acylation, halogenation and hydroxylation or were exploited as a metal ligand.[54] Remarkably, in contrast to alkylthiol derived sulphonic acids using grafting or co-condensation, these sulphonic acid groups were claimed to be thermally stable up to 500 °C. Such a thermal stability is certainly of importance in catalytic applications in the gas phase.[76b] Olefin moieties were also activated. The procedures involve electrophilic addition like bromination,[75] arylation,[81] amination,[82] hydroxylation,[83] or they include sequential reactions such as hydroboration–alcoholysis,[84] epoxidation-ring opening reaction,[84] or Diels–Alder-EAS-like reactions.[56,85] Due to the instable nature of some Si–C bonds (*vide supra*), careful handling during the post-synthesis treatments is a prerequisite. Si–C bonds underwent cleavage after hydroboration of vinyl organosilanes and subsequently applying an excess of alcoholysis reagent or mild oxidant, *viz.* NaOH–H_2O_2 or $NaBO_3{\cdot}4H_2O$.[84]

Multiple functionalisation and tuning of the functions has been realised by adding a second organosilane into the synthesis solution next to the bridged siloxane. Accordingly, distinct terminal or bridged organosilanes were mixed in a co-condensation solution, the balance between the two types of sites being controlled by their relative concentration. A controlled positioning of the respective functionalities is possible by integrating the organic moiety of the bridging organosilane in the pore wall and that of the terminal organosilane in the pore voids. The simultaneous introduction of bridging ethyl groups in the pore walls and protruding vinyl groups by co-condensation of bis(triethoxysilyl)ethylene and trimethoxyvinylsilane has already been reported in an early work.[77] Since then analoguous materials with an organic moiety inside the pore walls (*e.g.* as a bridging ethyl group) and another organic functionality protruding into the pore voids (*e.g.* amine, thiol, diamine, imidazole, pyridine, benzyl, phenyl ethyl groups, *etc.*) have been developed.[86,87] These bifunctional nanohybrids have been investigated for use in adsorption and separation.[88] In line with the co-condensation of end-group organosilanes and tetra-alkoxysilanes, the unit cell dimensions and pore size decrease with the loading of pendent organic groups.

The organic groups in the pores are more reactive in chemical reactions due to their better accessibility, while those in the pore wall exhibit exceptional physical, mechanical and hydrophobic/hydrophilic properties (*vide infra*).

2.2. Nanocomposites

The commercial implementation of nanohybrids is hampered by the cost of the organosiloxanes. The development of cheaper organosilanes should be helpful, but is challenging. Nanocomposites are often somewhat less defined materials that can be obtained from less expensive carbon sources such as existing resins and polymers like carbohydrates. Optional carbonisation of the nanocomposites, but also of the above-mentioned nanohybrids, yields special nanocomposites with pyrolytic carbon rather than with hydrocarbons next to silica.

2.2.1. Polymer based nanocomposites. In Fig. 2 the most successful strategies to introduce a polymer either in the pores (Fig. 2a and b) or in the pore wall (Fig. 2c) of OMS are summarised. One method leading to nanocomposites involves the

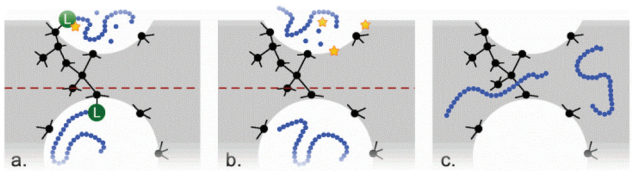

Fig. 2 Positioning of (functionalised) polymers in a nano-(hybrid)(composite); [a] inside the pore voids *via* covalent linking by polymerisation on a grafted linker/ initiator (*top*) or *via* immobilisation of a pre-synthesized polymer to a linker (*bottom*); [b] impregnation of monomers joint with an initiator (*top*) or a polymer (*bottom*); [c] in the pore wall *via* addition of the polymer (or monomers + initiator) to the synthesis gel. L = linker; Star = initiator.

impregnation with a prepared polymer (Fig. 2b, bottom) or with a monomer that is polymerised *in situ* using heat or an initiator (Fig. 2b, top). Covalent linkage is achieved by impregnation of a nanohybrid with immobilised monomer units or an anchored initiator (Fig. 2a, top). In agreement with the earlier definition, the latter materials are nanohybrids, although for the sake of clarity, they will be discussed in this section. Once the polymer is present in the OMS, it can be used directly in catalytic reactions if the polymer is functionalised or the polymer/silica composite serves as a precursor to form carbon/silica composites upon pyrolysis.

Impregnation of silica. The preparation of nanocomposites by impregnation of silica with polymers has received increased attention because of their potential use in catalysis. Early reports discuss the immobilisation of catalytically active inorganic polymers like heteropolyacids on silica gels,[89] as well as on OMS.[90] Likewise, organic polymers have been introduced *via* impregnation in various porous silica materials like OMS. With the impregnation technique, the organic polymer mainly resides on the internal and/or external surface of the silica rather than in the pore wall. Occasionally, OMS can be covalently bound to the polymer, provided the latter is carrying a coupling agent (Fig. 2a, bottom).[91] Alternatively, a nanohybrid decorated with an active polymerisation precursor – *i.e.* radical generator, monomer or transfer agent – can be used to induce polymerisation onto the OMS (Fig. 2a, top).[92]

Various methods consisting of one- or two-step procedures have been reported. The former synthesis involves an impregnation of OMS with the polymer, or an adsorption of the polymer (Fig. 2b, bottom). Deposition of DNA has been described.[93] A more detailed analysis of the location of the polymer reveals mainly deposition at the external surface, most probably because of the problematic diffusion of the macromolecules inside the pores.[94] The second method involves an impregnation, or an adsorption of the corresponding monomer, followed by a polymerisation triggered by heat or an initiator (Fig. 2b, top). Several silica materials like zeolites and OMS have been impregnated with aniline,[95] phenol/formaldehyde,[96] styrene,[97] vinylacetate,[97] acrylonitrile,[98] ethylene,[99] (methyl)methacrylate,[97,100] acrylamide,[101] furfuryl alcohol (FA),[102,103] and 4-vinyl pyridine,[104] followed by *in situ* polymerisation. The two-step approach is usually mentioned for the formation of nanowires and polymers with a controlled size, which find application in electronic nanodevices and meso-fiber synthesis, respectively. Catalytic applications with these polymer-based nanowires have not been reported at this moment.

Direct synthesis with polymers. Polymers may also be introduced directly in the initial synthesis gel. Mixing a polymer with TEOS, an ionic surfactant and NaOH results in a mesoporous nanocomposite with an entangled polymer/silica framework (Fig. 2c).[105] Isolated functional polymers have excellent catalytic properties, but suffer from a low surface area and thus limited accessibility. It was suggested that the spreading of the polymer over the inner pore surface area of silica could greatly enhance its effective surface area.[106] Accordingly, an increase of surface area of Nafion from 0.02 $m^2\ g^{-1}$ up to 50–153 $m^2\ g^{-1}$ was reported.[106] The choice of the silica source during synthesis influences the final polymer dispersion as well.[94] High ionic strength Na-silicate induces aggregation of Nafion polymer, while its dispersion is gradually improved by switching to Si-alkoxides. A recent successful synthesis with a non-ionic surfactant in acidic medium in the presence of polyacrylic acid enables the engineering of similar nanocomposites with larger pores up to 10 nm. With a classic ionic surfactant such as myristyltrimethylammonium bromide, only pores up to 2.5 nm can be achieved.[105b]

The as-prepared nanocomposites combine the catalytic properties of the organic polymer with the high surface area and the mechanical stability of the inorganic OMS. The obtained catalysts are highly stable in most common solvents, as leaching of the polymer is limited due to the strong entanglement in the framework.[94] To prevent decomposition of the polymer during synthesis – Nafion decomposes starting from 280 °C[107] – template removal is carried out by extraction rather than calcination. The use of an acidic extraction solution (*e.g.* 0.1 M H_2SO_4 in EtOH) not only allows retention of the pore ordering of OMS, but also regenerates the sulphonic acid groups attached to the polymer. To date, the successful incorporation of sodium poly(4-styrenesulphonate),[105c] Nafion,[94,105a] and polyacrylic acid[105b] into the silica pore walls has been reported.

Despite conservation of the polymer functionality, the amount that can be added to the synthesis gel, preserving the ordered pore structure and ensuring removal of excess of polymer, is limited.[105] The maximum incorporation of the polymer depends on its nature. In this respect, up to 20 wt% of Nafion has been occluded in MCM-41.[105c] The formation of a well ordered nanocomposite also depends on the chemical and structural properties of the polymer. Polystyrene sulphate strongly interacts with the ionic surfactant CTAB, as it forms a layered structure. As a consequence, the gradual transition of the layered to the hexagonal phase during the formation of siloxane bonds by condensation is hampered and the final pore ordering disturbed.[105c] Likewise, the homogeneous mixing of polymers in a hydrophilic solution with silica remains challenging. It was suggested that the presence of alkali ions enables the full miscibility of sodium polyacrylate in water,[105b] and that a strong ionic interaction of the cationic surfactant head and the anionic sulphate groups on the hydrophobic Nafion forces the polymer to reside in the aqueous phase.[105c] Moreover, the C–F bonds in Nafion are cleaved in the alkaline medium thus contributing to an increased hydrophilicity of the Nafion fragments.[105c] The catalytic applications of these porous nanocomposites with silica/polymer entanglement have been reported and will be further discussed in this review.

2.2.2. Pyrolytic carbon. Once an organic moiety is incorporated into the pore voids or framework of a mesoporous silica, carbonisation can be performed. Whereas all of the aforementioned nanohybrids and nanocomposites could be potential precursors, most research efforts have focused on the transformation of phenol resins,[108] or more recently on biomass derived organics like sucrose[5d,109] and FA[102,109–111] as

sustainable, cheap and abundant carbon precursors. The carbon precursor is introduced in the silica pore voids or silica pore wall by hard and soft templating techniques, respectively. Although polysaccharides such as starch have been used to prepare mesoporous carbons *i.e.* Starbon®,[112] their synthesis relies on self-assembly properties and the formation of mesoscopic metastable gel solutions. Tuning of the textural properties is obtained *via* a controlled gelatinisation (*e.g. via* temperature) of the polysaccharide.[113] Nevertheless their use as a carbon precursor in soft- or hard templated methodologies is yet to be reported. Both synthesis pathways have mainly been investigated in the search for novel ordered mesoporous carbon materials by removing the silica framework in HF solution.[4] Papers on the usage of (templated) mesoporous carbons in catalysis are numerous. Although a discussion on (ordered) mesoporous pure carbons is outside of the scope of this review, we want to stress their importance as closely related to the herein described nanocomposite catalysts, and therefore want to refer to relevant and high-impact reviews and articles offering a more in-depth discussion on the matter.[5–7] In contrast, reports covering the characterisation and catalytic application of the precursor composite material are scarce and thus this is the main subject of this review.

Depending on the nature of the organic carbon precursor, carbonisation is performed by heat treatment in an inert atmosphere, *viz.* pyrolysis of polyfurfuryl alcohol (PFA),[114] or under mild conditions at low temperature by chemical *viz.* H_2SO_4,[115] or hydrothermal treatment (*e.g.* sucrose).[116] Both thermosetting polymers, saccharides and even the structure directing surfactant[117] have been proposed as carbon precursor materials.[4] In fact, all non-thermally decomposable organic components are good candidates to be tested as a precursor. The final fraction of the carbon phase retained in the nanocomposite is determined by the carbon yield of the precursor. This value is highly dependent on the chemical nature of the organic precursor, such as the degree of volatile product formation, and its spatial environment during carbonisation.[4,118] Most block-copolymers have a very low carbon yield.[4] For example P123 has a limited carbon yield of 25 wt%, and is therefore not suitable for the formation of a silica/carbon nanocomposite.[118]

During carbonisation, heteroatoms are gradually expelled as CO, H_2O and CO_2 in the case of oxygen. The remaining polycyclic (hydro)carbon, carrying surface oxygen groups such as phenol and carboxyl groups, is gradually transformed into pure carbon material with only traces of oxygen and hydrogen (Fig. 3a). The extent of this transformation process and the degree of graphitisation depend on the chemical structure of the precursor and the thermal history such as the final pyrolysis temperature, the heating rate, *etc.* Polymers exhibiting a high degree of cross-linking like PFA have an increased resistance to graphitisation. Pyrolysis of these carbon precursors that are difficult to graphitise results in the formation of nanoporous carbon.[102,119,120] In other words, the careful selection of the carbon precursor and the carbonisation conditions enable a robust control of the physical (*e.g.* graphitisation degree, porosity) and chemical properties (*e.g.* functional groups) of the carbon component.

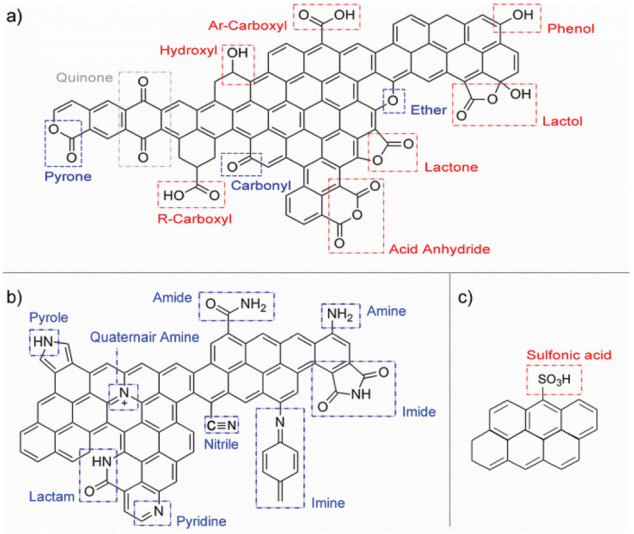

Fig. 3 Possible functional groups on a pyrolytic carbon surface as related to the presence of a heteroatom: (a) oxygen, (b) nitrogen and (c) sulphur. Basic and acid functionalities are indicated in blue and red, respectively.

In the previous polymer-based nanocomposites, the inorganic silica is responsible for the structural stability (*vide supra*). The pyrolysed carbon in the nanocomposite is very rigid and also contributes to the (hydro)thermal stability. Weakly bonded species like the unstable Si–C bonds, as in the nanohybrids, are absent. Hence these materials could find application in hot liquid water applications, in gas phase catalysis or other applications requiring harsh conditions.

As pyrolysis removes most of the oxygen atoms, there is a limited amount of surface oxygen containing functional groups that can be exploited as an anchoring or active site in catalysis. Many research groups therefore suggested an additional post-synthetic oxidation treatment. In general, these methodologies include a chemical oxidation agent such as HNO_3 or $Ca(OCl)_2$.[121] An alternative cheap and practical post-synthetic oxidation with air was found to increase readily the amount of surface oxygen groups.[110] Therefore, control of the treatment conditions – *i.e.* duration and temperature – is of utmost importance to avoid the extensive removal of carbon. In contrast, if partial carbonisation is chosen at pyrolysis temperatures ranging from 300 to 500 °C, a highly polycyclic aromatic carbon phase, containing multiple oxygen surface groups, rather than pure carbon is obtained. Further functionalisation of the aromatic rings can be accomplished by sulphonation (Fig. 3c). Starch is often preferred as the carbon precursor due to its high amylopectin content, giving a high yield of the required polycyclic aromatic rings.[122] In combination with the ability to adjust the carbon loading in the synthesis/impregnation solution, these tools enable control over the functional group density. Pure acidic carbons obtained from naphthalene, sucrose and starch demonstrate an improvement of the hydrothermal stability and a sulphonic acid group

density of 0.37 up to 1.34 mmol g^{-1} in comparison with mercaptopropyl derived sulphonic acids obtained by grafting (*vide supra*).[123] Contacting the aromatic rings with SO_3 vapour from fuming sulphuric acid[124] proved more efficient than chlorosulphonic acid,[50] or treatment with liquid concentrated H_2SO_4,[5d,125,126] as the final acid densities were much higher.

The introduction of nitrogen atoms and functional groups in the carbon framework is of much interest for the development of base catalysts. Post-synthetic functionalisation procedures, *viz.* N_2 and NH_3 cold plasma treatment or high temperature NH_3 handling, decorate the carbon component with a wide range of nitrogen functional groups (Fig. 3b), mainly as a result of the reaction with surface oxygen groups.[127] Pyrolysis of these carbons loaded with nitrogen functional groups or various nitrogen containing carbon precursors[128] results in nitrogen species incorporated into the carbon network as: (i) pyridine, (ii) quaternary nitrogen or (iii) nitrile functional groups.[129] The amounts of introduced nitrogen species are generally low as nitrogen-to-carbon ratios mostly reach up to 0.2.[129]

Hard templating. As the carbon precursor infiltrates the mesopores and consequently gets pyrolysed, the porosity can be readily tuned by varying the amount of carbon deposition as demonstrated for FA and sugars.[102,110,124,130] It was further demonstrated that by incipient wetness impregnation of FA a homogeneous carbon deposition occurs inside the silica mesopores. The subtle matching of the pore volume with the volume of the impregnation solution is key to direct the intraporous carbon deposition.[102,110] Moreover, the introduction of acid sites in the pore wall, *e.g. via* the isomorphous substitution of Si^{4+} by Al^{3+}, assists the *in situ* polymerisation inside the silica pores. This synthesis exemplifies the versatility of OMS for synthesizing new nanocomposites. Addition of a non-thermosetting solvent in the carbon precursor solution like mesitylene further controls the ultimate porosity of the materials. Mesoporous, biporous and microporous nanocomposite materials could be obtained from OMS.[102] The origin of microporosity was assigned to the formation of stacked graphitic nanocrystals, which are formed after high temperature pyrolysis and occluded in the matrix mesopores. Interestingly, the microporous structure induces shape-selective properties that can be exploited for the separation of linear and branched aliphatic isomers.[102] While microporosity is immediately generated even at low carbon loadings, its fraction gradually increases at the expense of mesoporosity.[102] Moreover, the pore size of the OMS template determines the final pore size distribution, influencing the shape selective behaviour, possibly through growth control of the size of the nanocrystals in the pore confinements of the OMS.[102b]

Sucrose is also used as a carbon source and tends to disperse homogeneously over the silica surface. Composites were obtained with pore sizes decreasing from 2.7 nm for parent MCM-48 down to 1.5 nm for a loading of 1.6 g sucrose g^{-1} MCM-48.[130] Whereas carbon is preferentially deposited inside the pores by capillary action, deposition on the external surface was avoided by controlling the carbon loading *via* the impregnation solution. If an excessive carbon loading is used, *viz.* above 50 wt% carbon in the nanocomposite, carbon is also deposited on the external surface of SBA-15.[131] Nitrogen adsorption experiments indicated preserved mesoporosity and a uniform coating of the inner silica wall at carbon loadings below 35 wt%. At higher sucrose loadings a gradual pore plugging occurred with a concomitant increase of the microporosity.[124,131] At high carbon loadings a high surface area was retained, which was assigned to the shrinkage of the carbon network during carbonisation due to the creation of voids between the mesopore walls and the carbon.[132] The gradual decrease in porosity also influences the functionalisation as high carbon deposition finally results in diffusion limitation of reagents during the activation process, reducing the total amount of active sites per unit weight of material.[124]

Recently ionic liquids have been examined as a carbon source in hard templating synthesis strategies. Their low vapour pressure enables cross-linking into a char without the loss of precursor molecules due to evaporation. Consequently ionic liquids have been transformed into carbons with a controlled, *via* specific cation–anion pairing interactions, porosity.[133] Accordingly, the bulk anions have been assigned a templating role in the creation of microporosity.[133] The addition of cross-linking functional groups combined with an increased thermal stability is crucial for the successful synthesis of porous carbons. Thermolysis properties are highly dependent on the chosen precursor.[134] The presence of nitriles in the anion or the usage of a N-based cation results in polymerisation after thermal decomposition.[135] The char forming nitrile not only allows the formation of a thermosetting polymer but also enables the direct synthesis of nitrogen functionalised carbon materials.[136] Confined carbonisation removes the restriction of the required cross-linking capability with regard to char formation by increasing the thermal stability of the ionic liquid.[137] Ionic liquids were introduced into the pore system of an inorganic oxide, *viz.* silica or titania, *via* a non-hydrolytic sol–gel synthesis procedure. Hard templating not only allows the synthesis of functionalised carbons *via* heteroatom containing ionic liquids but, in addition, enables tuning of the porous structure, as micro-, meso- or macroporous carbon(composites)s are obtained by varying the amount of ionic liquid trapped into the voids of the porous oxide.[137]

In order to produce mesoporous nanocomposites with carbon-like surface properties such as high hydrophobicity and an improved hydrothermal stability, mesoporous silicas have been coated with carbon after pyrolysis of: (i) the non-ionic surfactant,[118,138] (ii) benzene vapour,[139] (iii) grafted organic groups,[140] and (iv) low concentrations of sugar[130] (see section 3.1.2). In addition, pyrolysis of the surfactant significantly influences the final pore size of the mesoporous composite as the carbon avoids shrinkage of the silica framework. SBA-15 shows pore sizes of 6.8 nm, while the carbon filled analogue, *viz.* SBA-15/C, has pore diameters ranging from 7.3 to 7.9 nm. The extent of shrinkage ultimately depends on the rigidity of the carbon skeleton, which is determined by the pyrolysis temperature.[138] In contrast to the mesostructured

carbon synthesis strategy,[4,115] removal of silica is not necessary to obtain structurally stable mesoporous materials with carbon properties.

Soft templating. Although highly successful in certain cases, the hard templating method often suffers from a random distribution of the carbon constituent, pore blockage, phase separation and a disordered pore architecture. Furthermore, the nanocasting strategy is an expensive and time-consuming multi-step process. Finally, the mesoporous structure is often damaged during post-synthesis treatments.

Soft templating has been suggested as a valuable alternative method for the preparation of silica–carbon nanocomposites. Soft templating is commonly used for the synthesis of both OMS and ordered mesoporous carbons (OMC). While the use of OMS was discussed in the beginning of this section, the reader is referred to the reviews of Liang *et al.* and Chuenchom *et al.* for more details and an overview of recent progress regarding the synthesis of the OMC.[4,141] The first soft templating strategies used a bi-constituent synthesis solution comprising a surfactant and either a silica or carbon source to prepare OMS or OMC, respectively.

In general, the strategy relies on the self-assembly of template molecules such as amphiphilic surfactants or block copolymers, and the organic or inorganic building blocks. OMC have been prepared using polystyrene-poly(4-vinylpyridine),[142] polystyrene-poly(ethylene oxide),[143] or poly(ethylene oxide)-poly(propylene oxide) triblock copolymers (Pluronic family)[144] as the surfactant molecule and resol (phenol-formaldehyde, PF),[143] resorcinol-formaldehyde (RF),[142,144a,145] and phloroglucinol-formaldehyde (PGF)[144c] resins as the carbon precursor. To obtain a porous solid, the carbon precursor should be thermally more stable in comparison with the surfactant. Cross-linking of the carbon precursor is crucial for a successful OMC synthesis, as a rigid and stable carbon network is needed to endure surfactant removal and prevent pore collapse.[141] Phenolic resins thus greatly depend on the OH-content and the amount of formaldehyde which determine the degree of cross-linking and hence their final thermal stability.[141] Toward nanocomposite synthesis the presence of an additional inorganic component (*e.g.* silica) can overtake this framework supporting role (*vide infra*). The interaction between the template molecules and the carbon precursor (*e.g.* between OH groups in resins and PEO-chains in surfactant) is key for the successful synthesis of OMC by self-assembly. In this regard mono-, di- and tri-hydroxybenzene have been examined for the preparation of OMC, as they interact well with the PEO chains of the selected F127 block copolymer.[144c] If a carbon source with more hydroxylic groups was used, the mesoscopic ordering and surface area were significantly enhanced because of the enhanced hydrogen-bonding (S^0I^0 mechanism). Dai *et al.* demonstrated that successful OMC synthesis can also be accomplished under highly acidic conditions. As such, self-assembly is governed by electrostatic interactions of both the protonated OH groups of the C-precursor (I^+) and the protonated PEO blocks of the surfactant (S^+) with a counterion (X^-), thus allowing a $S^+X^-I^+$ self-assembly mechanism using polymeric resins while simultaneously accelerating the resin formation.[146] The final pore structure can be controlled *via* modifying the C-precursor to template ratio,[145,147] changing the fraction of hydrophilic PEO blocks in the surfactant,[147] using mixtures of surfactant molecules,[148] the cross-linking degree of the carbon precursor,[149] or by modifying the composition of the solution.[150] Accordingly, OMC with lamellar, hexagonal, cubic and disordered pore structures have been obtained. Similar to OMS synthesis strategies pore tuning can be accomplished *via* the usage of swelling agents such as homo-polystyrene as an expander molecule for micelles of polystyrene-poly(ethylene oxide),[151] or by increasing the size of the surfactant.[143,152] Increasing of the pore size goes together with a decrease of the thickness of the pore wall. OMC with pores up to 90 nm have been obtained but such an extensive enlarging of the pore size simultaneously results in multimodal pore size distributions and disordering of the pores.

The soft templating synthesis methodology has been extended to the synthesis of mesoscopically ordered nanocomposites by means of a tri-constituent co-assembly using a template molecule in combination with both the carbon and silica precursor. This approach enables the formation of mesoporous binary carbon–silica systems. While several of these nanocomposite materials have been synthesized, their use in catalysis remains unexplored, although their structural behaviour upon removing carbon or silica has been investigated. The role of the silica component is mostly limited to the prevention of framework shrinkage during pyrolysis. A drop in the mesopore size from 6.7 down to 6.0 nm was observed by decreasing the relative silica content in the pore wall. In the first report on the synthesis strategy using three distinct constituents, an organic carbon source, *viz.* PF, was added to a sodium silicate solution in the presence of a F127 template molecule.[153]

Using similar constituents such as resol precursor, TEOS and F127, mesoporous silica–carbon nanocomposites with large pores ranging from 6.0 to 6.7 nm, were prepared.[154] The self-assembly of the reagents was induced by an evaporation technique. This evaporation induced self-assembly (EISA) method is often preferred because it avoids the time-consuming hydrothermal processing involved in the templating synthesis.[155] Besides, the EISA synthesis strategy opens new pathways toward the synthesis of thin porous films. A variation on this strategy using an aerosol process with a silicate and phenolic oligomer in the presence of F127 was reported later.[156] Surfactant removal at 350 °C, optionally followed by a subsequent pyrolysis at 900 °C, resulted in silica/polymer and silica/carbon nano-composites, respectively. Carbonisation slightly increased the surface area due to the creation of micropores, while the mesopore size was reduced from 8 to 7 nm by framework shrinkage. A soft templated Si–C nanocomposite was first obtained by the EISA methodology using sucrose as the carbon source.[125,126] It demonstrates the high potential of the use of cheap and abundant biomass-derived carbon sources such as carbohydrates to produce mesoporous nanocomposites. Sucrose emerged as an ideal carbon source

because of its selective hydrogen bonding interactions with the polar EO blocks of the F127 triblock co-polymer.[125–126] As a result, a nanocomposite could be formed having entangled carbon and silica in the pore wall. The material has a hexagonally ordered pore structure with mesopores of 6.7–7.6 nm diameter.

Mesoporosity can only be created if thermally-degradable surfactants such as block copolymers F127 or P123 are used.[4] The final pore size is controlled by the length of the oligomer blocks in the surfactant and by the thermal conditions. Consequently these surfactants are often preferred over alkyl-chain-based ionic surfactants which have thermosetting properties,[4] unless the template is removed prior to pyrolysis.

In contrast, it was recently demonstrated that alkyl-chain-based ionic surfactants can be used successfully. Due to the similarity of the synthesis mechanism between RF and colloidal silica, a modified Stöber method was examined by replacing the common silica source by RF. This allowed for the synthesis of RF-derived carbon nanospheres from a solution comprising a basic catalyst, water/alcohol solvent in the presence of an ionic surfactant.[157] A polymer/silica/surfactant (PSS) composite was first prepared by a co-sol gel process of TEOS and RF in the presence of CTAB.[158] The morphology of the PSS could be modified by changing the ethanol-to-water ratio, resulting in the formation of rods and small and big spheres. As both RF and CTAB are thermosetting carbon precursors, remarkable hierarchical structures were obtained.

3. Catalytic exploitation of carbon properties

In the following section, the use of nanohybrids and nanocomposites in catalysis is discussed. The focus is on the importance of the carbon phase in the composite material in order to allow tuning of the physico-chemical properties towards performing catalysts. Each property will be discussed individually and its effect on catalysis will be illustrated with recent examples. Special attention is devoted to green and sustainable aspects of catalysis, such as immobilisation of catalysts, development of catalysts for aqueous reaction media,[159] synthesis of fine chemicals and catalytic conversion of bio-derived feedstocks.

3.1. Tuning of the catalyst pore size

The ability to control the pore size of a porous material is of high importance to ensure a high activity and selectivity in a catalytic reaction and to induce steric effects providing substrate specificity. For both PMO hybrids (Fig. 4A, i) and soft templated silica–carbon nanocomposites (Fig. 4C, ii) the organic moiety resides inside the silica wall, thus preserving the large mesopores, as provided by the OMS.

In contrast, for nanohybrid catalysts obtained by grafting (Fig. 4B) or co-condensation (Fig. 4A, ii) with terminal-end organo-silanes, and hard templated silica–carbon nanocomposites (Fig. 4C, i), the organic functionalities are positioned inside the pore voids, thereby inducing a reduction of the pore size.

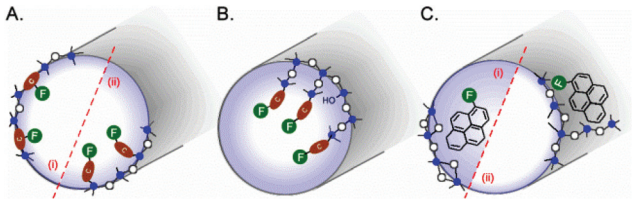

Fig. 4 Influence of the position of carbon components on the pore size of composite catalysts: (A) (i) condensation of bridging silsesquioxanes (PMO), (ii) co-condensation with terminal organosilane; (B) grafted OMS; (C) (i) hard and (ii) soft templated silica–carbon nanocomposites. F = organic functional group; C = organic moiety.

As the parent OMS template determines the upper limit of the pore size, its selection is crucial to guarantee satisfactory accessibility of the reagents to the catalytic sites. A large portfolio of ordered and disordered mesoporous silica is available, while various modifications of the synthesis procedures further extend the range of available pore sizes and morphologies (section 2). Even the disordered forms of OMS contain fairly uniform pores. The overall accessibility of OMS particles is determined by the mesopores size, the presence of interconnecting pores and the pore length (Table 2). Examples have been published showing their effect on the efficiency of the catalyst. A comparative study of the influence of the channel interconnectivity on mass transfer restrictions was performed for the selective oxidation of benzyl alcohol with molecular oxygen.[160] It was shown that the 3D sponge-like pore structure of TUD-1 suppresses mass transfer limitations that occur in the 1D and 2D pore structure of MCM-41 and SBA-15, respectively. Accordingly, the TUD-1 catalyst was most effective in the oxidation of benzyl alcohol. The particle morphology and the orientation of the mesopores towards the external particle surface determine the diffusion path length of reactants from the particle surface to the active sites.

Recently, attempts were made to prepare silica particles with a platelet morphology in which the mesopores are orientated perpendicularly to the external surface. The limited thickness of the platelets reduces the distance for molecules to reach the particle interior.[161] Variation of the Zr : TEOS and NaCl : TEOS ratios in a co-condensation with MPTMS yielded fibre, rod and platelet-like morphologies of amine functionalised SBA-15 with pore lengths of 10 μm, 600 and 200 nm, respectively.[161b] The as-prepared catalysts were examined in Henry reactions, Knoevenagel, and Claisen–Schmidt condensations (Fig. 5).[161] In the reaction of benzaldehyde with 2′-hydroxyacetophenone to form flavanone, the decreased diffusion distance significantly increased the observed initial TOF of the amine groups from 0.2 up to 8.3 h^{-1}, while the flavanone yield after 10 h of reaction at 140 °C increased from 48 to 72%. Alternatively, a reduction of the particle size is attempted, as in the Stöber method, allowing synthesis of nanospherical particles.[20] Such nanospheres of MCM-41 have been used as a hard template for the synthesis of a PFA derived nanocomposite.[110]

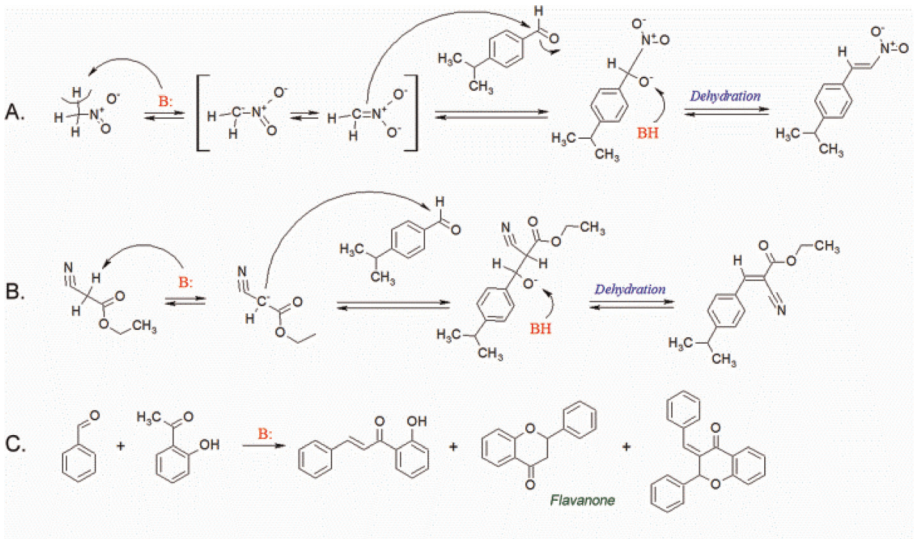

	NH_2-pr-SBA-15 grafted / Fibrous	NH_2-pr-SBA-15 co-condensation / Fibrous	NH_2-pr-SBA-15 co-condensation / Platelets
A (Henry reaction)	36.0 %	71.9 %	96.5 %
B (Knoevenagel reaction)	12.6 %	32.2 %	50.4 %
C (Claisen-Schmidt reaction)	-	39.8 %	92.0 %

Fig. 5 Catalytic reactions as examined using various SBA-15 catalysts as reported by Sujandi *et al.* (2008).[161a] Basic amine functionalities were introduced by grafting or co-condensation with APTES. The influence of the particle morphology was examined as fibrous (long diffusion distance) and platelet morphologies (short diffusion distance) were examined; reaction conversions for: (A) Henry reaction, (B) Knoevenagel condensation, and (C) Claisen–Schmidt reaction are given in the table.

Next to the unique incorporation and tuning of the bi-functionality and their cooperative effect (*vide infra* section 3.4), the short diffusion path in the small spherical particles was at the origin of the superior activity.[110]

3.1.1. Preservation of (meso)porosity. The preparation of silica–carbon composites by modifying an as-synthesized OMS can cause a reduction of the pore volume and diameter (*vide infra*, section 3.1.2). If the presence of larger pore sizes is a criterion for the absence of diffusion limitation in a catalytic reaction, the use of direct synthesis methods with bridging organosilanes leading to PMO (Fig. 4A, i) or of the soft templating method (Fig. 4C, ii) are recommended since these synthesis methods preserve the large pore dimensions, because the organic moiety is incorporated into the silica pore wall.

In view of catalytic applications, the chemical activation of PMOs was first reported by Nakajima *et al.*[85] Sulphonic acid groups residing in the silica wall were obtained after the attachment of aromatic groups to the ethylene bridging moiety *via* a Diels–Alder reaction and subsequent sulphonation (Fig. 6a).[56,85] The obtained PMO catalysts proved highly stable, as leaching of the sulphonate groups was limited when compared to those derived from thiol containing organosilanes. More interestingly, the pore diameter was only slightly reduced from 6.8 to 6.0 nm upon functionalisation,[85] hence providing sufficient accessibility of the catalytic sites. These PMO catalysts showed a high activity in the esterification of acetic acid and ethanol, as well as the Beckmann and pinacol rearrangement (Fig. 7).[56,85] On the other hand, benzyl-PMOs decorated

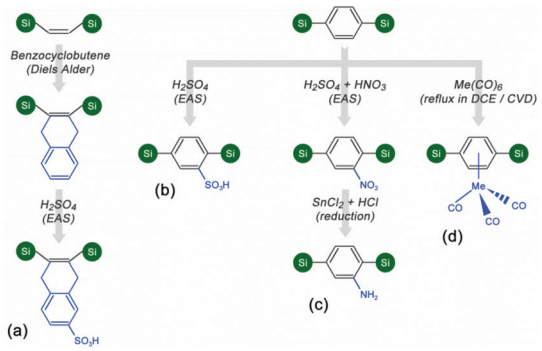

Fig. 6 Strategies for the indirect incorporation of functionalities in PMOs containing aromatic bridged organosilanes as applied for catalyst preparation.

with sulphonates (Fig. 6b),[76b] amines (Fig. 6b),[74] and metal complexes (Fig. 6c),[54,162] have been evaluated in various catalytic applications. However, next to the minimal reduction of the pore size, the specificity of these materials is based on the remarkable physical properties of their crystalline pore walls, which will be discussed in more detail in section 3.6.

Another remarkable PMO was obtained by co-condensation of bis[3-(triethoxysilyl)propyl]-disulphide and TMOS. The as-synthesized material presents a unique pore system. With an increase in the content of the silsesquioxane precursor, the 2D-hexagonal structure is gradually transformed into a cellular foam structure with large pores of 80 nm. Such pores allow fast diffusion of large reactants and products in the interior of

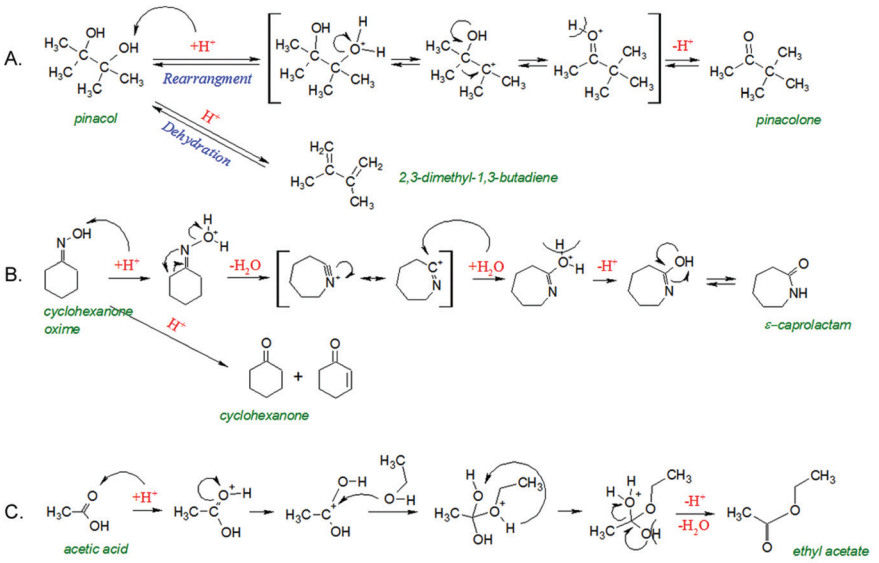

	A: Pinacol rearrangement *Conversion (Selectivity)*	B: Beckmann rearrangement *Conversion (Selectivity)*	C: Esterification *Reaction rate*
Nafion NR-50	42.2 % (88 %)	17.7 % (82 %)	1.2 μmol min^{-1}
H-ZSM-5	-	3.0 % (79 %)	-
H-Beta	-	8.8 % (77 %)	-
Amberlyst-15	69.5 % (84 %)	-	1.4 μmol min^{-1}
SO_3H-PMO	92.0 % (84 %)	31.6 % (79 %)	2.0 μmol min^{-1}

Fig. 7 Catalytic reactions examined using sulphonated PMO catalysts.[56,85] Reaction conversions, selectivities and rates for: (A) pinacol rearrangement, (B) Beckmann rearrangement of cyclohexane oxime, and (C) esterification of acetic acid are provided in the table.

the catalyst. Oxidation of the disulphide moiety resulted in a catalyst decorated with sulphonic acid groups in the pore wall.[55] As a consequence, high activities in the esterification of lauric acid could be achieved, attributable to the improved accessibility. Nonetheless, high organic moiety loadings strongly affected the mesostructure as the disulphide bonds constituting the pore wall were broken upon oxidation.

Soft templating avoids pore blocking and maximises the pore diameter created by surfactant template molecules since the latter are only removed after the introduction of the carbon.[117,126,163] The additional mixing of a carbon source in the synthesis gel allows excellent control of the final carbon fraction. Alternatively, the addition of an extra carbon source can be avoided by using a thermosetting surfactant. For instance, poly(ethylene oxide)-*b*-polystyrene (PEO-*b*-PS) was reported to function as a structure directing agent and a carbon source.[117] After hydrothermal aging, pyrolysis and sulphonation, a monohybrid catalyst with ultralarge pores up to 15 nm was obtained. Despite the limited acid densities of 0.03 mmol g^{-1}, in the condensation with ethylene glycol 93% of benzaldehyde was converted to 2-phenyl-1,3-dioxolane.

3.1.2. Reduction of pore size

Grafting. In the case of grafting, part of the internal voids are filled with organic moieties (Fig. 4B). Inherent to the procedure and in accord with the decrease in pore diameter, a concurrent drop in pore volume and surface area is generally observed upon grafting.[57,164] A careful selection of the size of the silylation agent permits fine tuning of the pore diameter, while occasionally the induction of shape selectivity has been reported. Next to reduction of the pore volume (size), conventional grafting sometimes results in a high packing density of the functionalities at the silica pore mouths. Sulphonic acid functionalised MCM-41 obtained by the grafting procedure showed significant lower activity in esterification of glycerol with lauric acid in comparison with catalysts obtained by co-condensation.[32] The hypothesis behind the reduced activity was pore blocking. In fact, increasing the acid content by coating instead of grafting did not increase the reaction rate. However, the reaction rate increased 3-fold at equal acid content by grafting a classic amorphous silica-gel instead of OMS.[32]

Grafting may thus inhibit efficient pore diffusion. While usually being a disadvantage for enhanced catalytic conversion, diffusion limitation may be exploited to immobilise very large active catalysts *via* non-covalent immobilisation strategies, for which otherwise the catalytic activity will be lost upon covalently linking the active site.[3b,165] Therefore, Venturello-like peroxophospho-tungstate anions, electrostatically attached to long chain alkyl chain cations in the inner voids of OMS, were found to be entrapped more effectively by

subsequent silylation and pore mouth size reduction, as no leaching was observed after washing of the catalyst.[166] The catalyst was active for the epoxidation of styrene and methyl oleate, showing epoxide selectivities up to 50%.[166]

Hard templating. Similar to grafting, hard templating comprises filling the OMS pore system with organics (Fig. 4C, i). Despite the reduction in pore size, the properties of the carbon fraction are highly advantageous for the stability and density of the acid groups. However, the activity of hard templated sulphonated composites presents a trade-off between porosity and acid density if bulkier substrates are involved in the chemical reactions. This issue has been demonstrated in the esterification of fatty acids and transesterification of triglycerides.[124,130]

Carefully controlling the amount of carbon deposition enables the conservation of an open pore system.[102,110,124,130] As a result, removal of the silica, required for the synthesis of mesoporous sulphonated carbon *via* hard template synthesis, can be avoided as it is time consuming, expensive and not environmentally benign. Moderate loadings of FA in MCM-41 and of sucrose in SBA-15 improved the activity of nanocomposite catalysts in the conversion of dihydroxyacetone into long chain alkyl lactates (Scheme 3),[110] and the transesterification of soy bean oil, respectively (Fig. 8).[124] Decreasing the sucrose loading from 35 to 25 wt% improved the conversion from 90 up to 99%, despite the lower acid site density.[124] The catalyst was further tested in the one-pot esterification/transesterification of industrial feeds containing fatty acids and vegetable oil from biodiesel production waste. Activities were barely affected, while a >98% ester yield was demonstrated for various palmitic acid concentrations.[124] The high concentration and the increased impurity degree of the fatty acid resulted only in a slightly decreased activity. The inhibiting effect of water is limited due to the hydrophobic microenvironment surrounding the sulphonic acid sites (see section 3.3.2).

3.1.3. Carbon induced (shape) selectivity. Grafting mesoporous silica generally reduces the average pore diameter according to the size of the organic moiety. In the case of mesoporous silica with relatively small pores, shape selectivity may be induced using sufficiently large silylating agents. Grafting presents a controlled method for engineering and tailoring pore sizes. Differences in the intraporous diffusion or size exclusion effects can appear after an additional decoration of the original OMS with active sites. Accordingly, a shape selective catalyst was prepared from small pore SBA-1 after a two-step grafting with triethyl aluminium and distinct long-chain alkyl dimethyl-aminosilanes, activating the OMS and tuning the pore size, respectively. The as-synthesized catalysts with pore sizes lower than 1.4 nm allowed discriminating between differently sized substrates in the Meerwein–Ponndorf–Verley reduction of aromatic aldehydes with 2-propanol.[167]

During a high temperature pyrolysis of a polymer filled OMS, amorphous carbon is formed which is gradually transformed further into graphite. The extent of this transformation relies on the degree of cross-linking in the polymer carbon precursor. In fact, highly cross-linked polymers are transformed into aromatic micro-domains that are connected by amorphous carbon. This misalignment of the graphitic domains induces microporosity with shape selective properties. Polymers such as PFA, polyvinyl(idene) chloride and polyacrylonitrile have been widely reported in the development of the so-called carbogenic molecular sieves (CMS).[168] Encapsulation and dispersion within the CMS matrix of catalytically active mesoporous silica/alumina has been reported.[169,120b] The resulting composite showed reactant and product selectivity in the reduction of alkenes and Fischer–Tropsch catalysis, respectively.[120b,169] In another example, dispersion of SiO_2–Al_2O_3 particles in a CMS matrix was used in the conversion of ammonia with methanol. A selectivity of 70% towards mono (MMA)- and dimethylamine (DMA) was reported, while the equilibrium selectivity in the applied conditions was predicted at 38% MMA–DMA selectivity. Clearly, the formation of trimethylamine (TMA) was delayed as a result of slow diffusion of TMA in the micropores of the carbon network (Fig. 9).[170] Moreover,

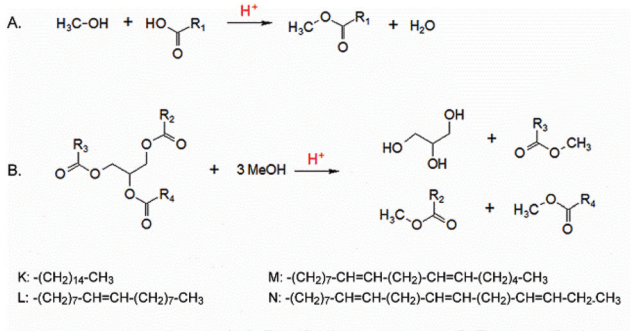

	A: Esterification *conversion (TOF)*	B. Transesterification *Yield*
Amberlyst-15	38.7 % (2.3)	40.9 %
Sugar-SO_3H	80.4 % (22.3)	88.9 %
CS-SO_3H (5%)	-	19.1 %
CS-SO_3H (15%)	-	85.0 %
CS-SO_3H (25%)	98,0 % (52.4)	99.0 %
CS-SO_3H (45%)	-	7.5 %

Fig. 8 (A) Esterification of palmitic acid (R_1 = K), and (B) transesterification of soy bean oil (R_2 = L, R_3 = M and R_4 = N), using a sulphonated hard-templated silica–carbon nanocomposite catalyst, *i.e.* CS-SO_3H (*x*) with various carbon loadings *x* (in wt%) demonstrating the influence of the pore size on the catalytic activity.[124]

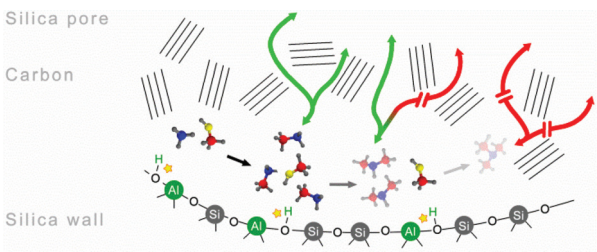

Fig. 9 Illustration of a microporous carbon (CMS) framework as a shape selective screen in the alkyl amine synthesis by acidic-CMS–silica/alumina nanocomposites. CMS induces the preferred synthesis of monomethylamine (MMA). The figure shows a cartoon of the catalyst pore.

the decrease of the acid site density is due to (i) the dissolution of the acid functionalities in the CMS matrix, and (ii) poisoning or decomposition of acidic sites during carbonisation. The catalyst was working much more slowly as compared with non-dispersed SiO_2–Al_2O_3, although its selectivity was significantly higher. High SiO_2–Al_2O_3 contents in the carbon matrix, *viz.* up to 80 wt%, resulted in a significant increase of the TMA yield due to the presence of acidic groups in those parts of the composite that are insufficiently covered with CMS. At high carbon contents (~45 wt%, obtained after two successive PFA/pyrolysis steps), MMA formation was in line with complete coverage of the catalytic sites with CMS, thus fully exploiting shape selectivity.

In the framework of adsorption experiments, additives like ethylene glycol have been added to bulk CMS materials to open the carbon framework with large transport channels.[120a] Application in catalysis and effects on the shape selective behaviour remain to be explored. Two research groups independently reported to have acquired CMS-like materials inside the pores of OMS using the hard templating technique. The aim was to keep the microporous properties of the carbon but to seriously reduce the diffusion distances as experienced in bulk CMS.[102,111] Actually, in commercial microporous carbon too slow transport of molecules occurs. Careful control of the concentration of FA in the impregnation solution, followed by a pyrolysis treatment, produces either mesoporous, combined micro- and mesoporous, or exclusively microporous composite systems.[102] The microporous materials were shown to exhibit unique shape selective properties in the separation of light gases and of linear and branched paraffins.[102] The bi-porous materials were chosen as a filler in the design of CO_2 reverse selective mixed matrix membranes because the outer silica phase optimises its dispersion in the polymer matrix. The high free-volume of the nanocomposite and the increased CO_2 affinity of the carbon surface resulted in superior flux/selectivity combinations in separating CO_2–H_2 gas mixtures.[171]

The presence of carbon in nanocomposites controls the access to the active site, not only for steric reasons related to the size of the reagents, but also due to the affinity of the support for the reagent molecules. Carbon-coated catalysts were obtained by contacting aggregates of small SiO_2 and TiO_2 particles, decorated with Pt nanoparticles (2–3 nm) and impregnated in a sulphuric acid solution, with FA vapour. The selectivity for CO in the oxidation of CO– H_2 mixtures (H_2–O_2–CO = 98 : 1 : 1) in excess of H_2 was significantly improved because of the preferential adsorption of CO by the carbon layer.[172] In addition, aggregation of Pt, sintering of the individual SiO_2/TiO_2 particles and phase transition of anatase to rutile were suppressed by the carbon coating, while the macro- and micropores were not eliminated during pyrolysis. As full carbon covering is crucial for selectivity, cracks were prevented by adding an organic template like tetrapropylammonium bromide to the impregnation mixture. The effect of the full carbon coating was illustrated for the oxidation at 125 °C. In comparison with non-carbon coated SiO_2–TiO_2 catalyst particles, the CO selectivity and conversion increased from 8 and 20% to 48 and 95%, respectively.[172]

3.2. Tuning of the surface area

Functional polymers greatly benefit from their incorporation in OMS. Indeed, despite the high activity of genuine polymers, they present low surface areas, especially when compared to OMS. Nafion, a perfluorinated sulphonic acid polymer, is often selected for exhibiting superacidic properties in combination with chemical and thermal stability. Attempts to impregnate the polymer on pre-formed OMS supports were unsuccessful due to the restricted accessibility of the interior for the macromolecules (Fig. 2b, bottom).

Polymer incorporation in the pore wall *via* sol–gel synthesis constitutes a preferred synthesis strategy. The resulting materials present a novel class of functional solid materials with sometimes drastically increased activity in catalytic conversions (Fig. 2c). Compared to impregnated and bulk polymer, Nafion/silica nanocomposites demonstrate up to 1000-fold increased activity (per unit weight of Nafion) as reported in various acid-catalysed reactions such as olefin isomerisation,[173] Friedel–Crafts benzylation,[174] α-methylstyrene (AMS) dimerisation,[105c,175] Fries rearrangement,[176a] esterification,[176b] acylation,[176c] and alkylation.[106] Pure Nafion is preferably used in polar solvents as it needs to swell to ascertain the accessibility of sulphonated groups. In contrast, the activity of a Nafion/silica composite is independent of the type of solvent due to the high dispersion of the sulphonic acid groups into the OMS framework.[175a] Consequently, the Nafion based composite catalyst may not only be applicable in non-polar solvents, but also under gas phase conditions.

Nafion/silica has been used in the dimerisation of AMS, resulting in the formation of the valuable unsaturated dimer products, *viz.* 4-methyl-2,4-diphenyl-1-pentene (molecular weight regulator) and 4-methyl-2,4-diphenyl-2-pentene (tetrachloromethane substitute), which may be transformed *via* an intramolecular Friedel–Crafts alkylation in the less valued bicyclic saturated dimer (Scheme 2). Nafion in amorphous silica gave relatively poor results toward the unsaturated

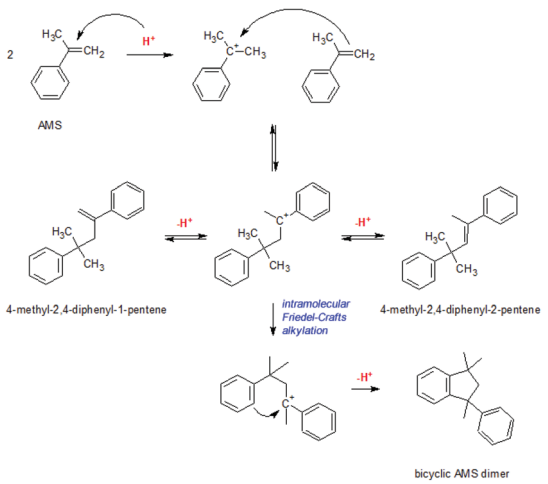

Scheme 2 Reaction scheme for the dimerisation of α-methylstyrene with an acid catalyst.

dimers. Modification of the reaction parameters, such as contact time and substrate concentration, increased the selectivity to the unsaturated dimer products up to 86% at 95% conversion.[175b] The use of the Nafion/MCM-41 catalyst yielded high amounts of the unsaturated dimer with negligible formation of the bicyclic saturated dimer (~4%).[105a,105c] This was explained by the performance of Nafion/MCM-41 in Friedel–Crafts (FC) reactions, which is highly dependent on the reaction temperature and substrate reactivity. At higher temperatures, FC reactions are possible as illustrated by the selective formation of the saturated dimer at 100 °C and by the competitive alkylations of benzyl alcohol with toluene/benzene[105a] or toluene/*p*-xylene.[105c] At lower temperature, *viz.* 70 °C, the activity and selectivity of Nafion/MCM-41 depends on the reactivity of the substrates. This was demonstrated by the respective yields of 1-methyl-2-(phenylmethyl)-benzene (37%) and 1,4-dimethyl-2-(phenylmethyl)-benzene (63%) that were obtained by the competitive FC reaction of benzyl alcohol with toluene and *p*-xylene, respectively, contrasting the equimolar product (50% yield) that was obtained using the Nafion/amorphous silica catalyst.[105c] Accordingly, the benzene ring of the unsaturated dimers is not reactive enough to Nafion/MCM-41 to complete the intramolecular Friedel–Crafts reaction, as it carries only one electron donating group to stabilise the carbocation intermediate, thus explaining the superior selectivity (Scheme 2).[105c]

Nanocomposites obtained through hard templating were shown to exhibit superior catalytic activities when compared to non-ordered carbon materials. This is due to the increase of the carbon surface area and accessibility of the active sites. Partially carbonised and sulphonated nanocomposite catalysts, obtained from SBA-15 filled with sucrose, showed a strongly increased activity and selectivity for the dimerisation of AMS.[131] The nanocomposite material was even more active in identical conditions (*vide supra*) than the catalyst comprising polymers inside the OMS pore wall. The authors suggested that a high carbon surface area is present since aggregation of the small individual carbon particles only occurs to a small extent. Enlargement of the carbon particle size, *e.g.* by using higher sucrose loadings, resulted in lowering of the catalytic turnover number. The authors assigned the efficient and selective production of the unsaturated dimeric pentenes from AMS to a synergistic effect of the sulphonic acid groups and the co-existent phenolic and carboxylic groups.[131] They found that the presence of silica, although important for its synthesis, is not crucial for the catalytic properties: after removing the silica, the remaining modified carbon retained the original high selectivity to the unsaturated dimeric pentenes. A sulphonated active carbon without phenolic and carboxylic acid groups was tested as a benchmark catalyst, showing poor catalytic activity and selectivity.

3.3. Tuning hydrophobicity

The degree of hydrophobicity of the catalyst surface is critical for the adsorption and desorption behaviour of substrates and (side)products. The latter two steps could affect in their turn the selectivity and activity of the overall catalytic process.

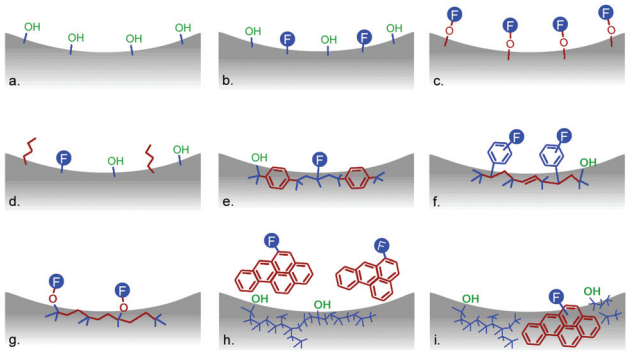

Fig. 10 Overview of synthesis strategies and their influence on the nature of the catalyst: Hydrophilic: (a) reference OMS, (b) organosilica by co-condensation; hydrophobic: organosilica by (c) grafting, (d–f) co-condensation, (g) combined co-condensation and grafting, or silica–carbon nano-composite by (h) hard or (i) soft templating. Functional groups contributing to the hydrophobicity or hydrophilicity are denoted in red and green, respectively. F = random organic functional group.

Although dependent on the conditions of the template removal, *i.e.* extraction or calcination temperature, OMS are in general considered hydrophilic due to the presence of surface silanols (Fig. 10a).[177] Removal or partial replacement of these silanols by grafting (Fig. 10c), or the addition of hydrophobic organic moieties inside the pore voids, *i.e.* by hard templating (Fig. 10h), or into the pore wall *via* direct synthesis *i.e.* co-condensation (Fig. 10b and d–f) or soft templating (Fig. 10i), induces a dramatic effect, as the hydrophilic silica can be switched into a highly hydrophobic composite catalyst.

3.3.1. Hydrophilic catalysts. Functionalisation of OMS can be beneficial for the conversion of large hydrophilic (bio)molecules. In fact, synchronizing the hydrophilicity of the catalyst and the reactants facilitates the adsorption of reactants on the catalytic surface. As a consequence, an increase of the conversion rate may be expected. Glycerol and hexitols such as sorbitol (D-glucitol) are of interest for further conversion into bio-derived chemical commodities.[178,179] Esterification of glycerol,[34,180] and sorbitol,[62,164] with fatty acids under mild conditions proceeds rapidly with sulphonated hydrophilic nanohybrid catalysts. The highest conversion rates were obtained with co-condensed instead of grafted nanohybrids (Fig. 7b), due to the higher loading, slightly increased hydrophilicity and better dispersion of the sulphonic acid active sites.[32,62]

Next to the conversion rate, the catalyst polarity may also influence the reaction selectivity. Not taking into account other determining parameters such as pore size, it can be stated that the concentration of a hydrophilic substrate in the pores should be higher for a hydrophilic catalyst. Accordingly, a difference in the hydrophilicity of two reactants could affect the reaction selectivity. Monoglycerides and glycerol monoethers present value-added chemicals. A complete esterification of glycerol with the fatty acids is undesired. In the biphasic reaction medium, a hydrophilic catalyst will reside in the polar glycerol phase, making the accessibility of the hydrophobic fatty acids to the catalytic sites problematic (Fig. 11A).

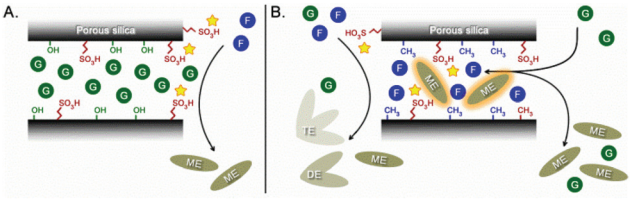

Fig. 11 Schematic representation of the use of organosilane-modified silica for esterification of glycerol (G) and fatty acids (F) to monoesters (ME): hydrophilic (A) and hydrophobic (B) organosilica nanohybrids; DE = di-ester and TE = tri-ester. Using strategy A, high yields were obtained for alcohol etherification (F = alcohol *e.g.* 1-phenyl-1-propanol) and esterification of hydroxylated fatty acids (*e.g.* F = juniperic acid).

Hence, poly-esterification will be reduced and monoglyceride formation preferred. In addition, undesired reactions of the fatty acids like dehydration and self-polymerisation, in the case of the usage of (hydroxylated) fatty acids such as juniperic acid, will be prevented. In addition, self-polymerisation is also avoided by the steric constraints at the active acid site.[180] The use of ionic surfactants with alkyl chains of various lengths during the nanohybrid synthesis (see section 2.1.2) further improved the monoglyceride selectivity of the co-condensated organosilica, demonstrating the importance of the pore ordering on the reaction selectivity.[181] In analogy, the etherification of glycerol with alcohols[182] or olefins[183] using hydrophilic nanohybrid catalysts was more selective towards mono-ether as compared to the more hydrophobic catalysts such as Amberlyst, sulphonated carbon, or the soluble *p*-toluene sulphonic acid (pTSA).

Selective monoglyceride synthesis is also achieved by a base-catalysed transesterification. The autocatalytic reaction of the fatty acid is now avoided, resulting in improved product selectivities with the basic nanohybrid catalysts compared to the acidic counterparts. As for the esterification reaction, the hydrophilicity of the catalyst controls the final product selectivity. In this regard, incorporation of an anchoring site for the basic active group such as 1,5,7-triazobicyclo[4.4.0]-dec-5-ene by co-condensation was suggested (Fig. 10b). Similarly, grafting of the anchoring group or applying an additional trimethylsilylation significantly reduces the monoester yield due to the increased hydrophobicity of the catalyst surface.[184]

3.3.2. Hydrophobic catalysts. Hydrophobic composite catalysts are preferred for reactions involving hydrophobic substrates, especially for the production of hydrophilic compounds. The concentration of the hydrophobic substrate in the catalyst pores will be high, while hydrophilic products like water will be expelled. Such sorption phenomena could be helpful in the case of equilibrium reactions such as esterification. It prevents catalyst deactivation due to strong interaction of the active site with water. The mesoporosity of the composites originating from OMS has also the advantage of rapid clearance and supply of chemicals in contrast to non-porous hydrophobic resins like Amberlyst-15.[57]

Grafting presents a common technique for increasing the hydrophobicity as it can replace the silanol groups by (apolar) organic functions (Fig. 10c and 1A). Next to the nature of the organic moiety, control over the grafting density enables tuning of the hydrophobicity (section 2.1.1). OMS catalysts grafted with MPTMS were more selective for the condensation of 2-methylfuran and acetone to 2,2-bis-(5-methylfuryl)-propane. Superior yields of 85% were obtained in comparison with more hydrophilic catalysts such as zeolites and co-condensed nanohybrids, because the oligomerisation of 2-methylfuran was depreciated.[62] If the active acid site is incorporated in the silica framework such as by isomorphous substitution of Al^{3+} for Si^{4+}, inactive hydrophobic silanes can be used. In the case of inactive OMS, grafting enables introduction of active acid sites, while a second grafting will allow altering the polarity of the catalyst. This dual grafting can even be performed simultaneously. So, SBA-15 was concurrently grafted with 3-aminopropyltriethoxysilane (APTES) and *n*-octyl silane. This nanohybrid catalyst was highly active in the hydrolysis of ethyl acetate after anchoring an acidic Keggin structure like $H_3PW_{12}O_{40}$ to the amino group.[46] Alternatively, a subsequent grafting with organosilanes – *i.e.* MPTMS and methyltrimethoxysilane – was performed to obtain a nanohybrid decorated with catalytically active sulphonic acid groups and methyl groups inducing hydrophobicity. The hydrophobicity of the catalyst has been demonstrated to improve the activity in the esterification of glycerol and lauric acid.[185] Finally, hydrophobic ionic liquids, *viz.* 1-methyl-3-octylimidazolium triflimide, have been adsorbed on sulphonic acid grafted silica gels.[186] The improved hydrophobicity was found beneficial in a Michael reaction,[186a] a Prins cyclisation, a cycloaddition and a dehydrative etherification.[186b]

Despite the presence of surface silanols, the direct synthesis of organosilica nanohybrids allows the development of hydrophobic catalysts by carefully choosing the organic moieties (Fig. 10d–f). Addition of propyltrimethoxysilane in a co-condensation with MPTMS or a perfluoroalkyl sulphonic acid silane improved the conversion rate in FC acylation reactions and the esterification of glycerol (affinity increase for the rather hydrophobic fatty acid, *i.e.*, lauric acid and expelling water) without loss of selectivity.[67,185] The effect of bridging organosilanes on the hydrophobicity of the catalyst has also been evidenced.[187] After replacing TEOS with 1,2-bis(trimethoxysilyl)ethane in a co-condensation with 2-(4-chlorosulphonylphenyl)-ethyltrimethoxysilane (CSPTMS),[187] enhanced dibutylether yields were obtained for the condensation of butanol. It was demonstrated that in this way the deactivation of the catalyst by water was significantly reduced. A similar approach for the synthesis of sulphonic acid ethane bridged PMOs catalysts was performed using either MPTMS or CSPTMS.[87d] The contribution of catalyst hydrophobicity to the acetalisation reaction rate of heptanal with 1-butanol was significantly larger compared to that of the acid strength. Analogous nanohybrid catalysts were prepared by co-condensation of MPTMS and 1,2-bis(triethoxysilyl)benzene. They were used in numerous organic transformations, *viz.* reaction of indole with benzaldehyde,[188] etherification of glycerol with 1-phenyl-1-propanol,[188] condensation of acetone and phenol,[87a]

hydrolysis of sucrose or starch,[87b] and esterification of acetic acid with ethanol.[87c] The improved activity and recyclability was assigned to a reduced solvation of the sulphonic acid groups in the hydrophobic environment. The use of an aromatic bridging group allows for the direct functionalisation of the PMO and makes the use of an additional organosilane in the synthesis gel obsolete. In this way, ethylene PMOs were developed and subsequently functionalised after arylation and sulphonation (Fig. 10e). The dual effect of retained mesoporosity (see section 3.1.1) and generated hydrophobicity resulted in very high activities for the self-condensation of heptanal.[81] Although the creation of surface silanol groups using the direct synthesis procedure counteracts hydrophobisation, they can be used during an additional grafting step to tune the hydrophobicity (Fig. 10g). A hydrophobic PMO, *viz.* ethane silica, was grafted with 1,2,2-trifluoro-2-hydroxy-1-tri-fluoromethyl-ethane sulphonic acid β-sultone (TFHTFMESS).[57] The final material is more hydrophobic compared to the original PMO and to the organosilane grafted OMS.[189] The grafting efficiency of PMO is often superior compared to that of pure silica, due to the improved diffusion of the silylation agent into the hydrophobic ethane silica.[57] Combining the improved hydrophobicity and the higher acid density results in a superior activity for the self-condensation of heptanal and its acetalisation with 1-butanol.[57]

Epoxidation presents an example of how a catalyst may benefit from an enhanced hydrophobic surface when hydrophobic substrates are converted into more hydrophilic products. In addition, hydrogen peroxide is the preferred oxidant as it is relatively cheap, readily available and produces only water as product.[190] Thus decomposition of H_2O_2 (by surface hydroxyl groups) is prevented and H_2O_2 selectivity improved.[37] The choice of the solvent (protic *vs.* aprotic or polar *vs.* apolar) or the oxidation agent (hydrogen *vs.* organic peroxide) strongly depends on the hydrophobicity of the catalyst surface.[191] Hydrophobic grafted Ti–silica catalysts were highly stable and demonstrated improved activities in polar protic solvents such as water and alcohol.[36,37,48] Alcohol or water can stabilise the active Ti-peroxo complex, rendering it more active as the electronegativity of the solvent decreases. Careful selection of the silylation agent is thus crucial as more efficient or less bulky silylation agents such as *N*-methyl-*N*-(trimethylsilyl) trifluoroacetamide[48] or trimethoxy-fluorosilane optimise the hydrophobicity and further improve the activity and selectivity.[49]

In accordance with hydrophilic nanohybrid catalysts, selective conversion of reagents can also be achieved with hydrophobic catalysts. The only prerequisite is that the reagents have largely distinct polarities such as in the etherification and esterification of glycerol with fatty acids. However, since these reactions involve water production and glycerol of the industrial grade contains a significant amount of water, hydrophobic catalysts are generally preferred. Selectivity is preserved if the fatty acids mainly reside in the catalyst and their self-polymerisation is hindered by pore confinement (Fig. 11B). Moreover, mono-functionalisation dominates because of the slow supply of glycerol. As it has been suggested that the organosilica catalysts are mainly active at the hydrophilic–hydrophobic interphase,[32] it is not surprising to see, after an initial conversion of glycerol, a steep catalytic activity boost as a result of the surfactant properties of the monoglyceride product, because the interphase area is strongly increased after reaching the critical micellar concentration.

The choice of a suitable organosilane is crucial for the selectivity and activity of the reaction and should not only be based on its hydrophobicity. An OMS grafted with TFHTFMESS showed superior esterification activities due to the higher acid strength.[189b] Nanohybrid catalysts obtained by direct synthesis of an alkyl organosilane and MPTMS demonstrated parallel steric constraints and activity drops, when the alkyl chain of the terminal organosilane is longer, especially for the larger substrates such as oleic acid *vs.* lauric acid (section 3.1.2). Furthermore, because of the decreased accessibility, most of the reactions occurred on the outer surface without steric constraints thus enabling multiple functionalisation and decreasing the selectivity.[185] The relative amounts of the organosilanes appeared to be crucial as high methyl trimethoxysilane contents next to MPTMS resulted in distinct thiol and methyl regions in the final catalyst.[50,185] Due to the close vicinity of the thiol groups, inactive disulphide species were preferentially formed,[67] and as a consequence the TONs dropped. To overcome this issue, the replacement of MPTMS by phenyl trimethoxysilane,[50] or 3-mercaptopropyl-(methyl)-dimethoxy-silane,[192] has been suggested.

3.3.3. Combined hydrophilic and hydrophobic catalysts. Soft templated silica–carbon nanocomposites comprise highly entangled silica and carbon phases inside their pore wall (Fig. 10i and 13, left). Accordingly, an alternation of hydrophobic and hydrophilic regions may exist at the catalyst surface. Activation of the polyaromatic carbon fraction allows the positioning of a catalytic function in a hydrophobic environment, while partially retaining a hydrophilic surface. This synthesis strategy is especially appealing for reactions with large hydrophilic substrates and a catalyst in which the catalytic sites are deactivated by a hydrophilic compound such as commonly occurs in acid-catalysed water mediated reactions. In this regard, sulphonated soft templated nanocomposites were used for the hydrolysis of cellulose to glucose (Fig. 12), yielding more than 50% glucose.[126,193] Adjacent hydrophilic regions stimulate the adsorption of β-1,4-glucan thus enhancing the hydrolytic activity.[126] The presence of

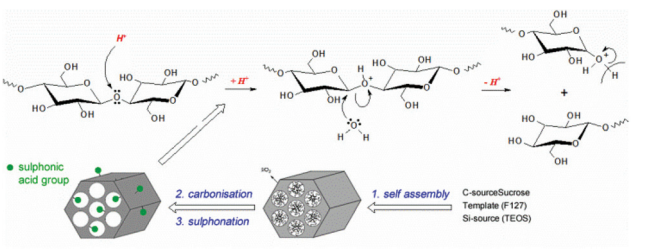

Fig. 12 Hydrolysis of cellulose to glucose using a sulphonated soft templated Si–C nanocomposite catalyst.[126]

carbon in the structure allows the formation of sulphonic groups at the outside of the nanocomposite particle, rather than exclusively inside the pores of nanocomposites as is the case with hard templating. These sites allow step-wise hydrolysis of large polysaccharide molecules into smaller sugars.

3.4. Multifunctionality

This section focuses on the use of nanocomposites (Fig. 13) and nanohybrids (Fig. 14) having multiple functional groups. Such multifunctional materials enable the development of cooperative effects in catalysis. For instance, tackling one-pot multi-step reactions requiring two chemically different active sites is made possible. The various synthetic strategies not only decorate the catalyst with multiple active sites, but also attempt a precise positioning of these active sites, leading to site compartmentalisation. The spatial resolution of the site control is important for the catalytic performance, as functional groups either need to be in close proximity, need to be separated to avoid a detrimental disturbance of the individual catalytic activities, or require positioning in an environment with distinct polarity.

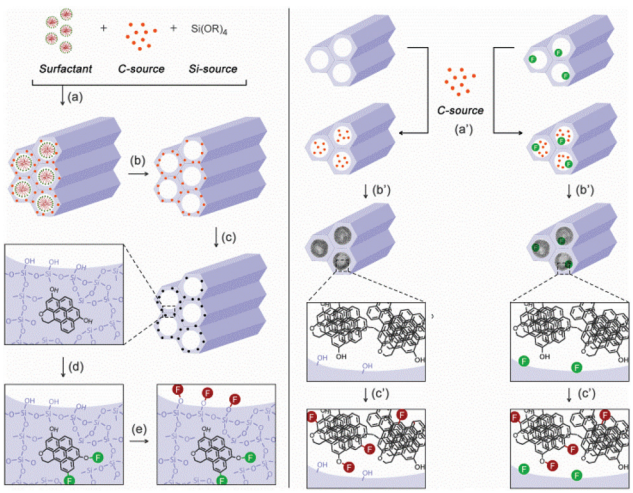

Fig. 13 Positioning of various catalytic sites (F) in a soft [left] and hard [right] templated silica–carbon nano-composite by component selective activation of the carbon fraction (*e.g.* AES) and/or silica (*e.g.* grafting). (a) Sol–gel synthesis, (b) extraction of template, (c) carbonisation, (d) functionalisation, (e) silica grafting; (a') impregnation, (b') carbonisation and (c') carbon functionalisation.

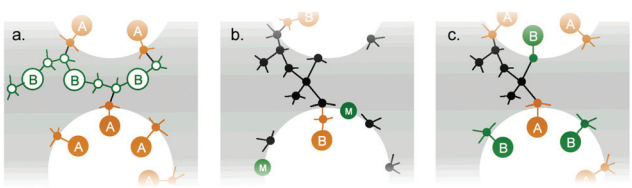

Fig. 14 Schematic overview of the positioning of multiple organic functional groups (A and B) in nanohybrids by: [a, c] co-condensation and [b] grafting of a pre-activated silica *e.g.* after decoration with metals (M). Tetra-alkoxysilanes (black), bridged silsesquioxane (white) and trialkoxyorganosilanes (full colour) are used as the (organo)-silane building blocks.

3.4.1. Spatial resolving of active sites

Compartmentalisation. Compartmentalisation involves the physical separation of different types of catalytically active sites. Such multifunctional systems are interesting in cascade reactions to obtain the maximum of each set of sites. In contrast, a cooperation effect is enabled when both types of active sites are homogeneously distributed over the catalyst surface.

Both soft (Fig. 13, left) and hard (Fig. 13, right) templated nanocomposites possess larger individual domains of each of the components, thus increasing their spatial distance in comparison with nanohybrid synthesis methods. Especially hard templated materials demonstrate a clear physical separation of the constituent phases in contrast to soft templated materials that still show entangling of the silica and carbon phases. As reports on soft templated materials in catalysis are rare, discussions are focussing on hard templated nanocomposites. As a result of incorporation of Al, Ti or Sn in the silica matrix, such materials are able to use catalytically active template material.

A bifunctional silica–carbon nanocomposite catalyst is produced after introducing an active organic component. In addition, if pyrolysed at high temperature, these catalysts are more thermally stable as compared to nanohybrid catalysts. Selective post-synthetic functionalisation of hard templated composites is hindered because either the silica surface is shielded by the carbon fraction or procedures like silylation cannot distinguish between the weakly acidic hydroxyl groups on both the silica and carbon surface. The carbon component is activated either by the presence of residual heteroatoms such as O and N or by additional functionalisation of the polycyclic aromatic carbon network (see sections 2.2.2 and 3.5.2). In order to obtain a catalyst consisting of a silica component decorated with Lewis acid sites at the inner pore wall, covered by a polycyclic aromatic carbon network comprising a high Brønsted acid density, the impregnation with FA of mesoporous silica grafted with well-dispersed Sn sites according to the strategy illustrated in Fig. 13 (right) has been suggested.[110]

The resulting multifunctional nanocomposite catalyst was highly active for the conversion of common sugars such as trioses and hexoses to added-value alkyl lactates or lactic acid,[194] in alcoholic and water medium, respectively. The high selectivity relies on the presence of Lewis acid sites, while weak Brønsted acidic sites improve the activity and TON of the Sn catalyst by assisting the transformation of trioses, *viz.* glyceraldehyde, into pyruvic aldehyde, a key intermediate. Optimisation of the content of weak Brønsted acid sites by changing the carbon deposition and applying a post-synthesis oxidation treatment further maximises the activity. The absence of strong Brønsted acids is crucial for selectivity reasons as they favour the formation of unwanted acetal products (Scheme 3). Isomerisation capacity of the nanocomposite catalyst proved rather low, which is a prerequisite to maximise lactate yields, when hexose substrates are envisioned. The additional retro-aldol reaction of the hexose governs the pathway for its further transformation *via* C_3 or C_4/C_2 fragments,[195] if performed on the ketose or aldose, respectively.

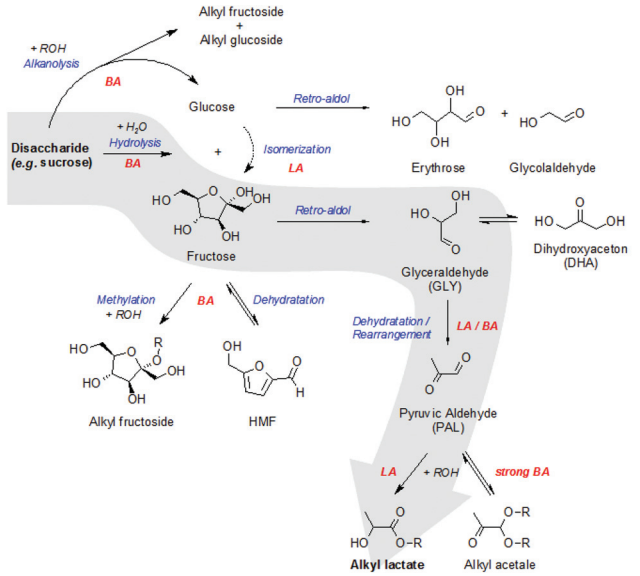

Scheme 3 Reaction scheme for the synthesis of alkyl lactates from common sugars in alcoholic or aqueous solvent. BA = Brønsted acid; LA = Lewis acid.

In accordance with microporous CMS,[168] decreased activities attributed to steric constraints were shown for longer alcohol substrates, to directly obtain long chain amphiphilic lactates, especially at high carbon loading.[102] The selective transformation of common sugars like glucose and sucrose were proven more sensitive to the balance of the acidic functionalities, because side-reactions such as dehydration and sugar methoxylation are abundant in the presence of Brønsted acids. They result in unwanted by-products like 5-hydroxymethyl furfural (HMF) and methyl glucose derivatives (Scheme 3). By altering the carbon deposition, pyrolysis temperature or by applying a simple post-synthetic oxidation, the previous example illustrates the ability to tune the catalytic site that is attached to the carbon fraction, independently of the active site located in the silica component.[110]

Spatial isolation of active groups. Alternatively, nanohybrids obtained by co-condensation of trialkoxy organosilanes and bridged silsesquioxanes contain functional groups at distinct sites, *viz.* in the pore voids and in the pore wall (Fig. 14a). This has been demonstrated using bistrimethoxysilyl-4,5-dithiooctane and APTMS.[196] Sulphonic acid groups were obtained after a consecutive reduction and oxidation of the disulphide moiety. Application of a similar strategy in catalysis showed that co-condensing a bridged silsesquioxane precursor such as 1,4-bis-(triethoxysilyl)-benzene and a trialkyl organosilane like aminopropyl trimethoxysilane (APTMS) results in sufficiently separated acid and basic functionalities, hence preventing their mutual deactivation.[197] The catalyst synthesis uses di-*tert*-butyl-dicarbonate protected amino groups, followed by sulphonation of the benzene linkers and amine deprotection. The acids and bases are located at distinct locations: the end group amine containing groups are directed in the pore, while the sulphonic acid groups are positioned in the pore wall (Fig. 14a).

In addition, the polarity of the nano-environments differs. The sulphonic acid groups reside in the hydrophobic part, while the amine functions are present in the hydrophilic part. The material was tested in a cascade deacetalisation–nitroaldol reaction to prove its ability for enzyme mimicking (Scheme 4). The benzaldehyde dimethyl acetal could be quantitatively converted into the nitrostyrene end product.[197]

Prior to a post-synthetic organo-functionalisation, OMS may be activated by isomorphous substitution or metal (ion) grafting. Grafting with metal ions instead of organosilanes preserves the presence of surface silanols, allowing further modification of the activated silica by silylation (Fig. 14b). Accordingly, the dual activation of SBA-15 was reported by subsequent grafting with Lewis acidic Ti^{4+} *via* reaction with tetrabutyl orthotitanate and various basic amines.[198] Alkylamine silanes were grafted directly on the Ti–silica surface, while guanine, imidazole and adenine required anchoring to a primarily grafted alkylchloride. The acid–base nanohybrid catalysts demonstrated a synergistic effect in the cycloaddition of CO_2 to epoxides because of the simultaneous activation of CO_2 and the epoxide by base and acid sites, respectively. Superior conversions and carbonate selectivities were obtained for the adenine grafted Ti–SBA in comparison with analogous catalysts prepared by avoiding the additional Ti-grafting step. Next

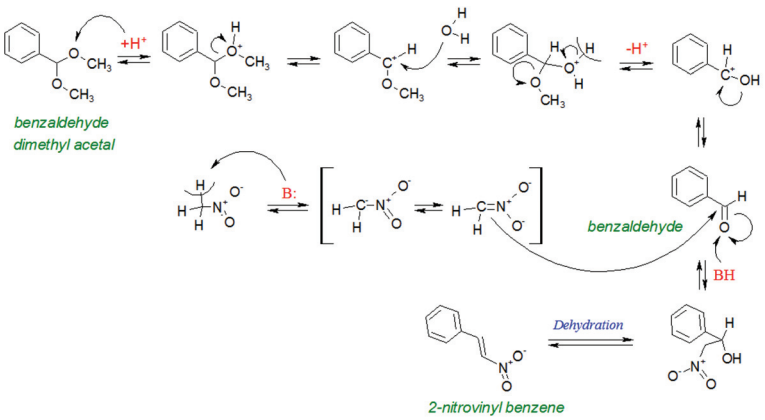

Scheme 4 Reaction mechanism of the cascade deacetalisation–nitroaldol reaction requiring both Brønsted acid (H^+) and base (B:) functionalities.

to the main product, *i.e.* the chloropropene carbonate, a minimal formation of diols or ethers was observed. Carbon dioxide, which is known to be activated by a solid base, could thus be exploited as a renewable raw material. An optimal CO_2 binding strength exists as stronger primary and weaker tertiary amines proved less active, compared to the secondary amine anchored to Ti–SBA.

3.4.2. Neighbouring active sites. The simple synthesis procedure of silylation allows the introduction of multiple functionalities in the final nanohybrid material. In its simplest form, two terminal organosilanes can be added in the desired amounts and ratios to fine tune the physico-chemical properties of the bifunctional nanohybrid catalyst (Fig. 14c). Various examples of such bifunctional catalysts have been reported such as thiols in combination with sulphonic acids,[51,199] or amine functional groups,[200] and sulphonic acids or weak acid silanols in combination with amines.[52,196,197,201]

The simultaneous immobilisation of acidic and basic functionalities challenges chemical transformations, requiring both basic and acidic catalysis. Such a combination is difficult to achieve in one-pot homogeneous catalysis. But even for heterogeneous catalysts, the possibility of mutual site neutralisation needs to be circumvented. Such bifunctional organosilicas were obtained *via* co-condensation of APTMS and 2-(4-chlorosulphonylphenyl)-trimethoxysilane with TEOS.[201a] The final nanohybrid catalyst comprised alternating acid and basic groups protruding in the pore voids. Its activity was examined for the aldol condensation of nitrobenzaldehyde and acetone. The reaction showed a fairly high conversion of 62% for the bifunctional catalysts, while the conversion rate was significantly lower for the analoguous monofunctional acid and base catalysts, yielding 16 and 33% conversion, respectively, after the same reaction time.[201a] The reaction mechanism comprises the formation of an electrophilic enolate by deprotonation of acetone, which then attacks the electron deficient aldehyde (Scheme 5). Hence the activity was correlated to the electronegativity of the aldehyde (Cl < F < NO_2 < CF_3) and the positioning (steric constraints) of the electron withdrawing group.[201b] Unfortunately, the authors noticed that the acidic and basic functions are transformed into ions during the enolate formation leading to mutual attraction and deactivation of the catalytic sites. Catalyst regeneration relies on the proton exchange between acid and basic groups. The importance of this exchange and the vicinity of both functions were illustrated by the addition of a co-solvent: apolar non-protic solvents such as hexane acquire a conversion of 88%, while only 23% conversion was observed in methanol. The limited formation of inactive ion pairs in hexane and the close association of the active sites are at the origin of the excellent conversion.[201a] A combination of weaker acidic organosilane such as a carboxyl group (with a pK_a of ~5) or a phosphoric acid (with a pK_a of ~3) with a strong primary amine base reveals complete conversion, because the reduced ionisation provides more active free acids and amines in comparison with the use of a sulphonic acid group (with a pK_a ~ −2).[201b]

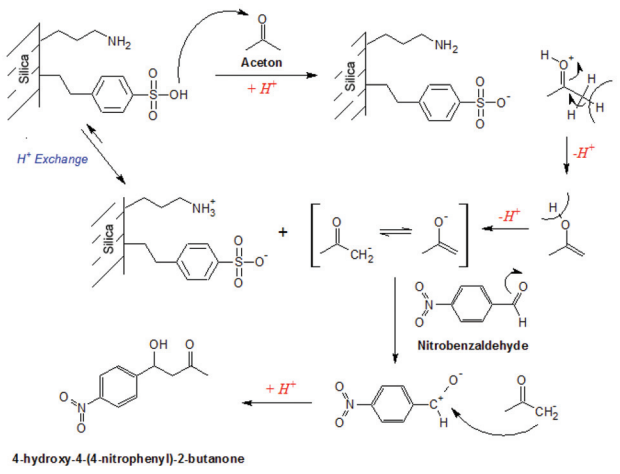

Scheme 5 Reaction scheme for the condensation of nitro-benzaldehyde and acetone by a bi-functional acid–base catalyst.

Based on steric hindrance of one of the active groups, an alternative method to prevent ion neutralisation has been developed.[52] Inspired by earlier work that demonstrated the superior activity of secondary amines for the condensation reaction,[202] a bifunctional organosilica catalyst was prepared carrying bulky secondary amine groups in combination with sulphonic acids.[52] A careful selection of bulky organosilanes is important to isolate incompatible active sites. The monofunctional hybrid catalyst decorated with secondary amines showed an increased conversion of 79% in comparison with primary amine attaining only 33%. A further conversion increase up to 94% for the bifunctional catalyst prepared with an anthracene moiety was assigned to the steric hindrance, preventing ion paring of the active groups.

Since aldol condensations preferentially proceed in the presence of weak acidity,[201b,203] one of the most straightforward synthesis strategies exploits the presence of the weakly acidic surface silanol groups of the silica component. Non-activated silica has proven to increase the catalytic activity of homogeneous amine catalysts in the aldol reaction of 4-nitrobenzaldehyde with acetone.[202] Heterogenisation of the amine catalyst was obtained by grafting the amino-containing silane onto the silica support. An increase of the catalytic activity was only noticed at low loading of the organic groups, which is in agreement with the preservation of residual silanol groups and their importance in the catalytic transformation.[204] Hence, for the formation of condensation catalysts, partial grafting at low temperature and in polar solvents should be considered to retain enough surface silanols. Similar nanohybrid synthesis strategies have been used to develop catalysts showing an improvement of the reaction rate in various other prototypical base-catalysed coupling reactions such as Henry[205] and Michael reactions.[205b] Interestingly, the length of the alkyl chain of the amino-containing silane determines the mobility of the amine group. If an alkyl chain of 3 or more carbon atoms is chosen, the mobility of the primary amines will be sufficient to approach the surface silanol, thus maximizing the

cooperative effect, as quenching of the active sites does not occur, in contrast to similar experiments with more reactive carboxylic acids.[206]

In summary, in order to exploit the cooperative effects of two incompatible functionalities either a physical separation or a minimal interaction is required.

Approximation of active sites. Sometimes, cooperative effects among catalytically active sites only appear when the two functional groups are brought in close proximity. The necessity for such a direct interaction has been encountered in the bifunctional condensation of acetone and phenol to bisphenol A (BPA) in the presence of both thiol and sulphonic acid groups. Mechanistically, the reaction comprises the activation of acetone by protonation prior to its attack by the thiol group, as the sulphur is highly nucleophilic. An electrophilic sulphonium intermediate is thus formed, which is more prone to attack the nucleophilic phenol. Experiments with homogeneous catalysts elucidated that, while mercaptopropane alone is not active, its addition to a sulphonic acid, *viz.* 1-propanesulphonic acid, is significantly increasing the BPA yield (based on total acetone conversion) from 11 to 44%, while the *p*,*p*′-isomer selectivity is being improved from 58 to 87%.[51] Catalyst heterogenisation was first attempted by a condensed monofunctional heterogeneous sulphonic acid catalyst in the absence of thiol functionalities. The nanohybrid catalyst showed a BPA yield of only 3.3%, while the addition of the soluble mercaptopropane improved the yield up to 13% (Fig. 15A). The importance of the neighbouring sites effect follows from the low BPA yield for a physical mixture of thiol and sulphonic acid functionalised SBA-15.[51] Bringing the thiol and sulphonic acid sites in close proximity was achieved by co-condensation as it ensures, in contrast to grafting (illustrated in Fig. 15B), a quasi-homogeneous distribution of the active sites (section 2.1.2).[199] Balancing of the thiol and sulphonic acid sites was done using various ratios of TEOS and/or 2-(4-chlorosulphonyl-phenyl)ethyltrimethoxysilane and MPTMS.[51] A maximal BPA yield of 74% and a superior selectivity of 95% (*p*,*p*′ : *p*,*p*′ + *o*,*p*′) were obtained at a 1 : 2 acid : thiol surface ratio (Fig. 15C), illustrating the importance of the close proximity of the thiol and sulphonic acid functional groups for the conversion and selectivity in BPA synthesis.[51] Analogous results were recently reported regarding the synthesis of diphenolic acid by the condensation of levulinic acid and phenol using sulphonated hyperbranched polymers in the presence of soluble thiols. Mechanistic investigations allowed us to conclude that the smallest thiol is most beneficial for the rate increase, while the isomerisation between the regioisomers of diphenolic acid should be avoided in order not to shift the *p*,*p*′ to *o*,*p* ratio towards the thermodynamic value.[207]

Site pairing presents a strategy to acquire the regular and close positioning of distinct active sites at the molecular level.[208] The strategy comprises grafting or condensation with a nano-engineered organosilane that, after its decomposition by thermal[199] or chemical modification,[209] comprises multiple organic functions. This way, SBA-15 was grafted with either an asymmetric or symmetric disulphide or disulphonate ester.[199] After oxidation, the symmetric disulphide (Fig. 16A) proved most active even compared to the stronger aryl sulphonic acids, as the incomplete oxidation of the mercapto functionalities (section 2.1.1) results in the close positioning of thiols and sulphonic acid groups.[199] Since the partial oxidation cannot be controlled, a sultone group was grafted on a silica substrate.[209]

The sultone-ring opens upon attack by a nucleophilic agent such as a thiol anion. Consequently, both a thiol and sulphonic acid are formed. The choice of the nucleophile, *i.e.* a thiol anion or a monoanionic dithiol with various chain lengths, provides a lever to subtly tune the distance between the thiol

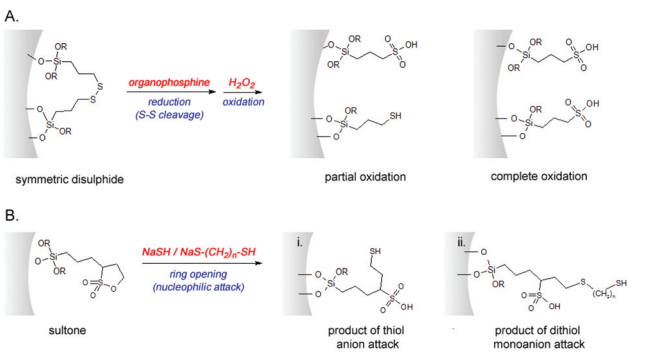

Fig. 16 Strategies for site-pairing of thiol and sulphonic acid groups to optimise BPA synthesis using nanoengineered organosilanes. (A) Symmetric disulphide, (B) sultone.

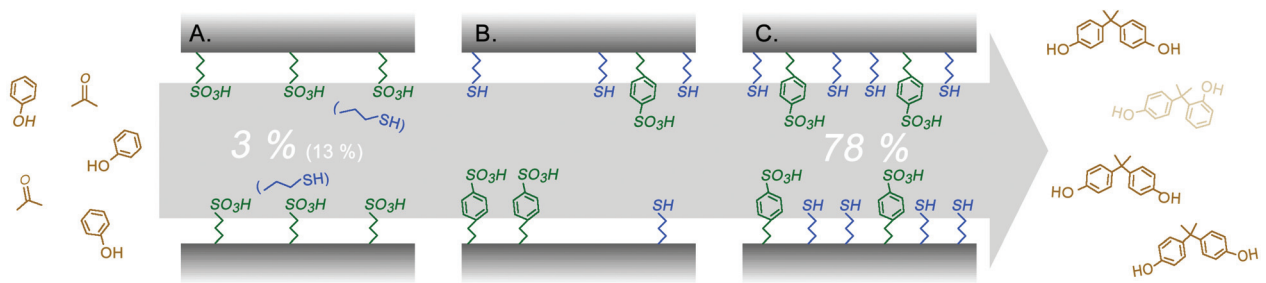

Fig. 15 Effect of the cooperation of thiol- and sulphonic acid groups on the bisphenol-A yield (indicated in %) based on full acetone conversion, using: (A) a monofunctional (sulphonic acid) acidic organosilica (in parentheses the effect of the addition of homogeneous mercaptopropane on the conversion) or a bifunctional (sulphonic acid and thiol) organosilica obtained by (B) grafting or (C) co-condensation.

and sulphonic acid functional groups. The thiol anion (Fig. 16B, i) is superior, resulting in a per site yield of 83%, which is in the same range as that of the optimised co-condensation procedure (82%) (*vide supra*). The dithiol nucleophile (Fig. 16B, ii) appeared less efficient, resulting in a gradual decrease of BPA yield when the dithiol monoanion chain length is extended.[209]

3.5. Metal active sites

3.5.1. Metal impregnation. Acquiring a high metal dispersion on OMS using conventional impregnation of metal salts proves challenging (Fig. 17a).[210,211] As a consequence, various carbon-based solutions have been suggested in the literature to reduce metal migration and sintering effects.

For instance, the creation of an interruption of the silica pore wall with hydrophobic carbon zones improves the metal dispersion, since the metal ions are adsorbed on the silica component, while the hydrophobic carbon conserves their separation (Fig. 17b). Transport of metal precursors is thereby reduced and aggregation is prevented, when compared to impregnation of a bare OMS material. Such an alteration of hydrophilic and more hydrophobic regions in the silica wall was obtained for soft templated nanocomposites after high temperature pyrolysis of a carbon precursor such as phenolic resin (Fig. 13, left).[163] The average nanoparticle size can be minimised (3.5 nm) in comparison with the pure silica (10.6 nm) and polymer (8.2 nm) supports. In combination with mesoporosity and increased hydrophobicity, a highly active catalyst for C–C coupling reactions such as Heck and Ulmann reactions in water was obtained.[163] Next to the composites, pure carbon materials such as activated mesoporous carbon could present an alternative as a support material, and in fact, even smaller metal particles (2.1 nm) were acquired using CMK materials. This is due to the presence of micropores in which the metal can nucleate after intrusion of the metal salt solution, induced by capillary forces (Fig. 17d).[163] However, because of the decreased accessibility of the metal particle, such carbon catalysts have a lower activity, while activated carbons suffer from a broad pore size distribution, hence inducing heterogeneity of the size of the metal clusters. One may conclude that composites are useful support materials to obtain high metal dispersions *via* impregnation techniques.

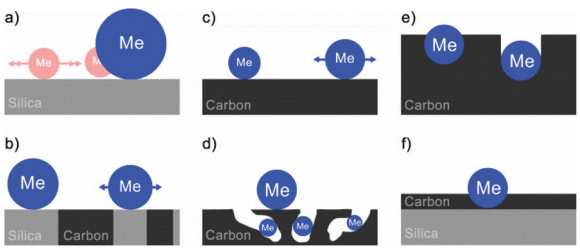

Fig. 17 Schematic presentation of the metal (Me) dispersion on various supports after impregnation with a metal salt solution and its subsequent chemical (H_2 or hydride) (a–d) or thermal reduction (e–f).

The reduction step for impregnated OMS usually results in weakly bound metal species with an enhanced mobility, thus promoting sintering. Alternatively, metal precursors deposited on a carbon surface can be reduced by a thermal reduction method under an inert atmosphere as the reduction involves an interaction between the carbon and metal.[212] Metal particles are obtained semi-embedded in a concave carbon surface. The latter is electron poor due to the coincidental electron density shift after a configuration change of part of the carbon atoms from sp^2 to sp^3.[213] Such a unique nano-environment was reported for Ru deposited on carbon coated silica (Fig. 17f).[212] A strong interaction, related to the electron donation of Ru to the carbon surface, prevented oxidation, leaching and aggregation of the metal nanoparticles. In contrast, Fe^{3+} could not be reduced by the thermal treatment using a similar approach.[214]

The presence of an electrically highly conductive carbon component as support could prove beneficial as illustrated in various redox reactions. Thus, NH_3 decomposition was significantly enhanced using Fe_2O_3 particles deposited on carbon coated SBA-15 because of the improved electron transfer from the active site to the reactant, hence facilitating the recombination and desorption of N_2.[214] Likewise, Ru deposited on carbon coated OMS showed a high activity toward the hydrogenation of benzene and toluene.[212] The authors claimed that after H_2 chemisorption on Ru, a hydrogen spill-over effect from Ru to the carbon phase, where the hydrophobic olefins are expected to be adsorbed, occurs. The embedding of Ru induced by thermal reduction, as described above, further increases the interphase interaction between metal and carbon. More hydrogen transport channels are present in accord with the superior activity. When the composite is treated in the presence of hydrogen or when only the silica part is used, a decrease of catalytic activity was observed due to a reduction in interphase contact.[212] Extensive embedding should be avoided since it will lead to accessibility issues (Fig. 17e).

3.5.2. Anchoring metal complexes. Many strategies have been proposed for the covalent anchoring of complex active species to a wide range of support materials. The anchoring sites are commonly constituted by amines, thiols, cyanides or carboxylic groups. Often OMS is chosen as a support because of its large mesopores and high surface area.[198] Examples are countless and outside of the scope of this review. For instance, over the past two years, the anchoring of various metal complexes (Sn, Pd, Zr, Ni, In, *etc.*) on silica gel grafted with APTES has been reported. The catalytic performance of these nanohybrids was examined in distinct organic transformations such as the Mannich reaction, Suzuki–Miyaura coupling and Pechman condensation.[45] More details of this strategy can be found in an extensive review of immobilisation of homogeneous catalysts.[165a,215]

In general the alteration of the chemical environment of the active complex upon immobilisation is undesired because of a potential drop in the catalytic activity in comparison with the native active complex. Nevertheless, encouraging effects on

the catalytic activity have also been reported. For instance, the TOFs of a Mn–salen complex immobilised on SBA-15, grafted with either alkyl thiols or sulphonic acids, increased for the selective oxidation of terpenes with air in comparison with the free complex.[198] This was assigned to a lowering of the oxidation state of Mn (from 3+ to 2+) due to the immobilisation procedure. The increased stereoselectivity for the oxidation of the olefinic bond of limonene followed the variation in electron density and oxidizability of the Mn ions, which seem to be related to the nature of the anchoring site. Hence immobilisation of the complex on thiol or sulphonic anchoring groups resulted in 1,2-epoxide selectivities of 100 and 82%, respectively.[198]

3.6. Physico-chemical stability

Although being highly versatile and promising catalytic support materials, amorphous OMS catalysts suffer from a low thermal and mechanical stability, particularly when exposed to moisture (Fig. 18A). Structural collapse occurs when contacted with water at elevated temperature or after compression.[216] Next to thickening of the silica wall,[13a,217] or an increase of the framework condensation,[218] hydrophobisation is a well-known tool to improve the preservation of the silica integrity: water is repelled avoiding hydrolysis of Si–O–Si bonds.[38,61c,217,219] The low mechanical stability involves a mechano-chemical process in which adsorbed water molecules affect the structure on impact of pressure.[220] Composites of OMS show an increased thermo-mechanical stability. They can be obtained by co-condensation (Fig. 18B, i), grafting (Fig. 18B, ii), condensation (Fig. 18C) organosilica synthesis procedures using hydrophobic organosilanes or *via* hard templating of OMS (Fig. 18D) performed at sufficiently high pyrolysis temperatures (section 2.2.2).

Post-synthetic hydrophobisation of OMS was achieved by grafting.[38] Replacement of surface silanols by trimethylsilyl groups on *e.g.* MCM-41 and MCM-48 greatly increased the overall stability against moisture or external pressure (Fig. 18B, ii). The stability increase strongly depends on the nature of the silylation agent. The persistence of the organosilica in aqueous solutions improved using hexamethyldisilazane instead of trichloromethylsilane.[219a] Remarkably, after calcination of the trimethylsilylated silica, the stability was still improved, thus suggesting the formation of various types of siloxane bonds with distinct stabilities.[38] Incorporation of identical trialkoxy-organosilanes *via* the direct synthesis method showed lower hydrothermal stabilities compared to grafting. The lower stability was ascribed to the less condensed silica wall and the presence of hydrophilic surface silanols in the case of the direct synthesis method (Fig. 18B, i).[61c] Although grafting and co-condensation might be effective in improving stability, they also affect the porosity and chemical surface properties of the material.[217]

Next to the polarity issue, also the degree of crystallinity plays a role in the stability of nanocomposites and nanohybrids. By condensation of a proper bifunctionalised silsesquioxane such as 1,2-bis(triethoxysilyl)benzene, a very stable PMO is formed with a highly crystalline pore wall (Fig. 18C). The as-synthesized PMO nanohybrid material presents a unique surface structure as hydrophilic and hydrophobic properties, originating from the silicate and benzene layers, respectively, are periodically arranged.[76b] Taking into account the stability and the presence of mesopores, these phenyl-PMO are highly interesting materials for catalytic applications. Although most reports focus on the regular ordering, pore size and hydrophobicity with regard to their performance, one should bear in mind that also the stability will contribute to their industrial processing potential. Various functionalisations have been suggested to acquire ordered mesoporous organosilica catalysts, while retaining the crystalline pore wall, AES being such a flexible functionalisation tool. Both basic and acidic functions have been attached to the phenyl moiety with this technique.[74,76b] Amine decorated phenyl PMOs, obtained by a two-step nitration/reduction protocol (Fig. 6c), proved highly stable and selective in Knoevenagel condensation, as malononitrile and benzaldehyde were quantitatively converted into 1,1-dicyanophenyl-ethylene.[74] The phenyl moiety has also been partially complexed with carbonyl ligated Cr or Mo after chemical vapour deposition,[54] or liquid phase contacting (Fig. 6d)[221] using the corresponding hexacarbonyl metal complexes. Polymerisation of phenylacetylene and dehydrochlorination of 2-chloro-2-methylbutane show that the catalytic activity of the immobilised complexes strongly

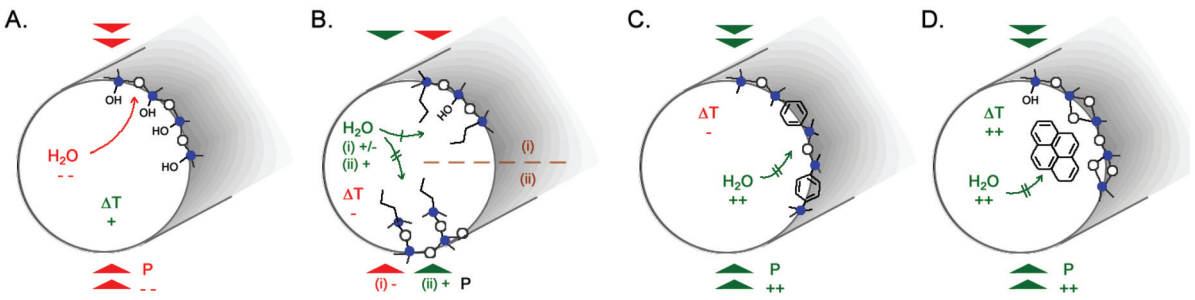

Fig. 18 Influence of the organic component on the stability of an OMS-based catalyst: (A) OMS, (B) organosilica obtained by (i) co-condensation or (ii) grafting with a hydrophobic organic moiety, (C) phenyl-PMO, and (D) hard template silica–carbon nanocomposite. Shown is a detail of the (modified) silica pore. P = Pressure; T = temperature. Green/red colour and +/−: The colour code indicates whether the composite is stable (green) or not (red). An arbitrary indication of the degree of its stability (+/−) is given as well.

depends on the bond strength between the metal centre and the phenylene ligand. In contrast to Cr, Mo binds relatively weakly with the phenylene moiety, enhancing its partial dissociation and thus resulting in a superior activity.[54]

Despite its higher stability, nanohybrids or nanocomposites remain sensitive to thermal treatment. The instability of the Si–O–C bond or even the more stable Si–C bond poses great challenges to the regeneration of the catalyst. Removal of unwanted side-products inhibiting the active sites without altering or destroying the active organic function proves challenging. For instance, the nanohybrid – *i.e.* perfluoromethyl β-sulphone grafted OMS – esterification catalysts could easily be regenerated by washing with ethanol. However, the acylation activity of the catalyst is inhibited by the adsorption of carbocationic intermediates. Regeneration by high temperature desorption is blocked as, despite being more stable as compared to sulphonic acid groups obtained after oxidation of thiols (300–350 °C), the silyloxy bond proves instable at temperatures above 350 °C.[189b] Alternative silylation agents have been suggested to allow the synthesis of more stable organosilica catalysts decorated with perfluorinated sulphonic acids.[222]

The absence of the Si–O–C or even Si–C bonds and the harsh synthesis conditions render silica–carbon nanocomposites more stable (Fig. 18D). Nonetheless, the carbon structure is also altered by thermal treatment under inert conditions such as desorption of CO and CO_2 due to decomposition of functional groups or oxidative environments.[110] Therefore the thermal regeneration of the catalyst needs to be precisely controlled.

In addition, the chemical stability of the active function could depend on its position within the pore system. The metal-free oxidation of glycerol to ketomalonic acid after immobilisation of 2,2,6,6-tetramethyl-1-piperidinyloxy (TEMPO) on an amino-functionalised silica has been reported.[223] Incorporation of the amino groups by co-condensation allows for the anchoring of the TEMPO complexes deeply within the pore system due to the homogeneous introduction of the organic moiety (*vide supra*). The authors suggested that the positioning of the complex within the sol–gel cages of the silica could be attributed to the improved stability of the solid catalyst using the co-condensation method[223] instead of grafting.

4. Conclusions and outlook

Because of the ever increasing economic and environmental demands, the necessity of complex multi-step reaction schemes requiring the contribution of multiple active sites has become a topical research area. Moreover, many current catalysts are instable in hot water. Mixing homogeneous or heterogeneous catalysts is not feasible as the ecological requirements are not met or because harmful interactions and long diffusion distances between the active sites restrict the overall catalytic performance. Although intelligent heterogeneous catalyst design, involving nano-engineering of support and active sites, presents a profound solution to tackle these challenges, it requires an expansion of the current catalyst design tools.

In this review various examples are discussed illustrating the wide range of synthesis and modification tools offered by inorganic–organic nanocomposites and nanohybrids, and the impact of such modifications on their catalytic performance. These composites comprise two chemically different phases which are adaptable with many nano-engineering techniques to introduce active sites, to control their position and to tune the chemical and physical properties of the micro-environment.

The physico-chemical properties of the nanohybrids, comprising a covalent bond between the inorganic and organic phase and obtained by direct or grafting methodologies, are mainly determined by the selection of the organosilane and the way it is incorporated into the final material. Changing its amount or nature enables tuning of hydrophobicity, active site strength, pore sizes and crystallinity and makes possible the introduction of multiple active sites, either well-dispersed or isolated in compartments. Recent advances of such an organo-modification consist of the development of more complex designs such as the use of multifunctional organosilanes by thorough pre-synthesis engineering. The potential of such organosilanes lies in the control of a precise positioning of the active sites at a molecular scale resulting in optimisation of cooperative effects in catalysis.

Research on the catalytic performance of hard and soft templated nanocomposites is mostly related to the hydrophobicity and size effects, but also to site location, demonstrated with some catalytic examples. Although somewhat less advanced in their molecular design, these catalysts could present a more cost-effective alternative to the nanohybrids. Selective functionalisation techniques in combination with the spatial resolution of both phases in hard templated composites offer new possibilities to deal with cascade reactions, for which avoidance of unfavourable interactions between the different active sites is crucial. Soft-templated nanocomposites show pore walls with entangling of silica and carbon. Such a composition allows exploitation of the approximation concept of distinct catalytic sites, possibly inducing cooperative effects. As discovered in nanohybrid research, transfer of the multifunctionality concepts to nanocomposite design could be inspiring for the design of future nanocomposite catalysts.

Acknowledgements

The authors thank the Flemish Government (Methusalem program) and the Research Council of the KU Leuven (IDO – 3E090504) for their funding. F.d.C. is grateful to the Belgian Science Policy (BELSPO) for providing financial support in the framework of the IAP (Interuniversity Attraction Poles) network. S.V.d.V. thanks the Research Foundation – Flanders (FWO) for a postdoctoral fellowship and acknowledges support from the Belgian American Educational Foundation (BAEF)

and the Fulbright Commission for Educational Exchange between the United States and Belgium. M.D. acknowledges FWO (grant 1.1.955.10N) for financial support.

Notes and references

1 G. Kickelbick, *Hybrid Materials. Synthesis, Characterization, and Applications*, Wiley-VCH Verlag GmbH & Co. KGaA, Weinheim, 2007.
2 M. Nanko, *AZojomo*, 2009, **6**, 1–8.
3 (*a*) A. Stein, B. J. Melde and R. C. Schroden, *Adv. Mater.*, 2000, **12**, 1403–1419; (*b*) A. P. Wight and M. E. Davis, *Chem. Rev.*, 2002, **102**, 3589–3614; (*c*) F. Hoffmann, M. Cornelius, J. Morell and M. Froba, *Angew. Chem., Int. Ed.*, 2006, **45**, 3216–3251; (*d*) A. Corma and H. Garcia, *Adv. Synth. Catal.*, 2006, **348**, 1391–1412; (*e*) Q. Yang, J. Liu, L. Zhang and C. Li, *J. Mater. Chem.*, 2009, **19**, 1945–1955; (*f*) F. Hoffmann and M. Froba, *Chem. Soc. Rev.*, 2011, **40**, 608–620.
4 C. Liang, Z. Li and S. Dai, *Angew. Chem., Int. Ed.*, 2008, **47**, 3696–3717.
5 (*a*) X. Wang, R. Liu, M. M. Waje, Z. Chen, Y. Yan, K. N. Bozhilov and P. Feng, *Chem. Mater.*, 2007, **19**, 2395–2397; (*b*) R. Xing, Y. Liu, Y. Wang, L. Chen, H. Wu, Y. Jiang, M. He and P. Wu, *Microporous Mesoporous Mater.*, 2007, **105**, 41–48; (*c*) R. Liu, X. Wang, X. Zhao and P. Feng, *Carbon*, 2008, **46**, 1664–1669; (*d*) L. Peng, A. Philippaerts, X. Ke, J. Van Noyen, F. De Clippel, G. Van Tendeloo, P. A. Jacobs and B. F. Sels, *Catal. Today*, 2010, **150**, 140–146; (*e*) J. Janaun and N. Ellis, *Appl. Catal., A*, 2011, **394**, 25–31; (*f*) L. Geng, G. Yu, Y. Wang and Y. Zhu, *Appl. Catal., A*, 2012, **427–428**, 137–144; (*g*) B. Chang, J. Fu, Y. Tian and X. Dong, *J. Phys. Chem. C*, 2013, 130313140244001.
6 (*a*) V. L. Budarin, J. H. Clark, R. Luque and D. J. Macquarrie, *Chem. Commun.*, 2007, 634–636; (*b*) R. Luque, V. Budarin, J. H. Clark, P. Shuttleworth and R. J. White, *Catal. Commun.*, 2011, **12**, 1471–1476.
7 R. T. Mayes, P. F. Fulvio, Z. Ma and S. Dai, *Phys. Chem. Chem. Phys.*, 2011, **13**, 2492–2494.
8 F. Goettmann, A. Fischer, M. Antonietti and A. Thomas, *Angew. Chem., Int. Ed.*, 2006, **45**, 4467–4471.
9 C. T. Kresge, M. E. Leonowicz, W. J. Roth, J. C. Vartuli and J. S. Beck, *Nature*, 1992, **359**, 710–712.
10 (*a*) B.-C. Chen, H.-P. Lin, M.-C. Chao, C.-Y. Mou and C.-Y. Tang, *Adv. Mater.*, 2004, **16**, 1657–1661; (*b*) S.-Y. Chen, C.-Y. Tang, W.-T. Chuang, J.-J. Lee, Y.-L. Tsai, J. C. C. Chan, C.-Y. Lin, Y.-C. Liu and S. Cheng, *Chem. Mater.*, 2008, **20**, 3906–3916; (*c*) L. Cao and M. Kruk, *J. Colloid Interface Sci.*, 2011, **361**, 472–476.
11 (*a*) J. Jammaer, A. Aerts, J. D'Haen, J. W. Seo and J. A. Martens, *J. Mater. Chem.*, 2009, **19**, 8290–8293; (*b*) J. Jammaer, T. S. van Erp, A. Aerts, C. E. Kirschhock and J. A. Martens, *J. Am. Chem. Soc.*, 2011, **133**, 13737–13745.
12 (*a*) Q. Huo, R. Leon, P. M. Petroff and G. D. Stucky, *Science*, 1995, **268**, 1324–1327; (*b*) W. Zhou, H. M. A. Hunter, P. A. Wright, Q. Ge and J. M. Thomas, *J. Phys. Chem. B*, 1998, **102**, 6933–6936.
13 (*a*) D. Zhao, J. Feng, Q. Huo, N. Melosh, G. H. Fredrickson, B. F. Chmelka and G. D. Stucky, *Science*, 1998, **279**, 548–552; (*b*) Y. Sakamoto, M. Kaneda, O. Terasaki, D. Y. Zhao, J. M. Kim, G. Stucky, H. J. Shin and R. Ryoo, *Nature*, 2000, **408**, 449–453.
14 F. Kleitz, D. Liu, G. M. Anilkumar, I.-S. Park, L. A. Solovyov, A. N. Shmakov and R. Ryoo, *J. Phys. Chem. B*, 2003, **107**, 14296–14300.
15 C. Yu, Y. Yu and D. Zhao, *Chem. Commun.*, 2000, 575–576.
16 H. I. Lee, J. H. Kim, G. D. Stucky, Y. Shi, C. Pak and J. M. Kim, *J. Mater. Chem.*, 2010, **20**, 8483–8487.
17 (*a*) S. Inagaki, Y. Fukushima and K. Kuroda, *Stud. Surf. Sci. Catal.*, 1994, **84**, 125–132; (*b*) T. Ishikawa, M. Matsuda, A. Yasukawa, K. Kandori, S. Inagaki, T. Fukushima and S. Kondo, *J. Chem. Soc., Faraday Trans.*, 1996, **92**, 1985–1989.
18 J. S. Beck, J. C. Vartuli, W. J. Roth, M. E. Leonowicz, C. T. Kresge, K. D. Schmitt, C. T. W. Chu, D. H. Olson and E. W. Sheppard, *J. Am. Chem. Soc.*, 1992, **114**, 10834–10843.
19 (*a*) C.-F. Cheng, D. Ho Park and J. Klinowski, *J. Chem. Soc., Faraday Trans.*, 1997, **93**, 193–197; (*b*) B. Pauwels, G. Van Tendeloo, C. Thoelen, W. Van Rhijn and P. A. Jacobs, *Adv. Mater.*, 2001, **13**, 1317–1320.
20 M. Grün, I. Lauer and K. K. Unger, *Adv. Mater.*, 1997, **9**, 254–257.
21 (*a*) M.-C. Chao, D.-S. Wang, H.-P. Lin and C.-Y. Mou, *J. Mater. Chem.*, 2003, **13**, 2853–2854; (*b*) C.-C. Ting, H.-Y. Wu, A. Palani, A. S. T. Chiang and H.-M. Kao, *Microporous Mesoporous Mater.*, 2008, **116**, 323–329.
22 (*a*) V. Alfredsson and M. W. Anderson, *Chem. Mater.*, 1996, **8**, 1141–1146; (*b*) M. Widenmeyer and R. Anwander, *Chem. Mater.*, 2002, **14**, 1827–1831; (*c*) K. Schumacher, M. Grün and K. K. Unger, *Microporous Mesoporous Mater.*, 1999, **27**, 201–206.
23 R. Ryoo, J. M. Kim, C. H. Ko and C. H. Shin, *J. Phys. Chem.*, 1996, **100**, 17718–17721.
24 S. A. Bagshaw, E. Prouzet and T. J. Pinnavaia, *Science*, 1995, **1**, 1242–1244.
25 J. C. Jansen, Z. Shan, L. Marchese, W. Zhou, N. v. d. Puil and T. Maschmeyer, *Chem. Commun.*, 2001, 713–714.
26 (*a*) W. Zhang, T. R. Pauly and T. J. Pinnavaia, *Chem. Mater.*, 1997, **9**, 2491–2498; (*b*) T. R. Pauly, Y. Yu Liu, T. J. Pinnavaia, S. J. L. Billinge and T. P. Rieker, *J. Am. Chem. Soc.*, 1999, **121**, 8835–8842.
27 A. B. D. Nandiyanto, S.-G. Kim, F. Iskandar and K. Okuyama, *Microporous Mesoporous Mater.*, 2009, **120**, 447–453.
28 (*a*) X. S. Zhao, G. Q. Lu, A. K. Whittaker, G. J. Millar and H. Y. Zhu, *J. Phys. Chem. B*, 1997, **101**, 6525–6531; (*b*) N. Fukaya, H. Haga, T. Tsuchimoto, S.-y. Onozawa, T. Sakakura and H. Yasuda, *J. Organomet. Chem.*, 2010, **695**, 2540–2542.

29 L. T. Zhuralev, *Langmuir*, 1987, **3**, 316–318.
30 W. Kolodziejski, A. Corma, M. Navarro and J. Pérez-Pariente, *Solid State Nucl. Magn. Reson.*, 1993, **2**, 253–259.
31 R. K. Iler, *The Chemistry of Silica: Solubility, Polymerization, Colloid and Surface Properties, and Biochemistry*, Wiley, New York, 1979.
32 W. D. Bossaert, D. E. De Vos, W. M. Van Rhijn, J. Bullen, P. J. Grobet and P. A. Jacobs, *J. Catal.*, 1999, **182**, 156–164.
33 D. Das, *J. Catal.*, 2004, **223**, 152–160.
34 F. Jérôme and J. Barrault, *Eur. J. Lipid Sci. Technol.*, 2011, **113**, 118–134.
35 R. Anwander, I. Nagl, M. Widenmeyer, G. Engelhardt, O. Groeger, C. Palm and T. Ro, *J. Phys. Chem. B*, 2000, **104**, 3532–3544.
36 M. B. D'Amore and S. Schwarz, *Chem. Commun.*, 1999, 121–122.
37 T. Tatsumi, K. A. Koyano and N. Igarashi, *Chem. Commun.*, 1998, 325–326.
38 K. A. Koyano, T. Tatsumi, Y. Tanaka and S. Nakata, *J. Phys. Chem. B*, 1997, **101**, 9436–9440.
39 V. Ayala, A. Corma, M. Iglesias, J. A. Rincón and F. Sánchez, *J. Catal.*, 2004, **224**, 170–177.
40 I. Dominguez, V. Fornes and M. Sabater, *J. Catal.*, 2004, **228**, 92–99.
41 C. Mukhopadhyay and S. Ray, *Tetrahedron*, 2011, **67**, 7936–7945.
42 A. Martín, G. Morales, F. Martínez, R. van Grieken, L. Cao and M. Kruk, *J. Mater. Chem.*, 2010, **20**, 8026–8035.
43 Y. Kubota, H. Ikeya, Y. Sugi, T. Yamada and T. Tatsumi, *J. Mol. Catal. A: Chem.*, 2006, **249**, 181–190.
44 C. Piovezan, R. Jovito, A. J. Bortoluzzi, H. Terenzi, F. L. Fischer, P. C. Severino, C. T. Pich, G. G. Azzolini, R. A. Peralta, L. M. Rossi and A. Neves, *Inorg. Chem.*, 2010, **49**, 2580–2582.
45 (*a*) R. K. Sharma and C. Sharma, *J. Mol. Catal. A: Chem.*, 2010, **332**, 53–58; (*b*) R. K. Sharma and C. Sharma, *Catal. Commun.*, 2011, **12**, 327–331; (*c*) R. K. Sharma, A. Pandey and S. Gulati, *Appl. Catal., A*, 2012, **431–432**, 33–41; (*d*) R. K. Sharma, D. Rawat and G. Gaba, *Catal. Commun.*, 2012, **19**, 31–36; (*e*) R. K. Sharma and D. Rawat, *Inorg. Chem. Commun.*, 2012, **17**, 58–63.
46 K. Inumaru, T. Ishihara, Y. Kamiya, T. Okuhara and S. Yamanaka, *Angew. Chem., Int. Ed.*, 2007, **46**, 7625–7628.
47 T. Sakai, Y. Tsutsumi and T. Ema, *Green Chem.*, 2008, **10**, 337–341.
48 J. Bu and H.-K. Rhee, *Catal. Lett.*, 2000, **65**, 141–145.
49 T. Kamegawa, N. Suzuki, K. Tsuji, J. Sonoda, Y. Kuwahara, K. Mori and H. Yamashita, *Catal. Today*, 2011, **175**, 393–397.
50 J. n. Pérez-Pariente, I. Díaz, F. Mohino and E. Sastre, *Appl. Catal., A*, 2003, **254**, 173–188.
51 R. Zeidan, V. Dufaud and M. Davis, *J. Catal.*, 2006, **239**, 299–306.
52 Y. Shao, J. Guan, S. Wu, H. Liu, B. Liu and Q. Kan, *Microporous Mesoporous Mater.*, 2010, **128**, 120–125.
53 D. Esquivel, C. Jiménez-Sanchidrián and F. J. Romero-Salguero, *J. Mater. Chem.*, 2011, **21**, 724–733.
54 T. Kamegawa, M. Saito, T. Sakai, M. Matsuoka and M. Anpo, *Catal. Today*, 2012, **181**, 14–19.
55 C. Li, J. Liu, L. Zhang, J. Yang and Q. Yang, *Microporous Mesoporous Mater.*, 2008, **113**, 333–342.
56 K. Nakajima, I. Tomita, M. Hara, S. Hayashi, K. Domen and J. N. Kondo, *Catal. Today*, 2006, **116**, 151–156.
57 D. Dubé, M. Rat, W. Shen, F. Béland and S. Kaliaguine, *J. Mater. Sci.*, 2009, **44**, 6683–6692.
58 A. Corma, M. T. Navarro, F. Rey, V. R. Ruiz and M. J. Sabater, *ChemPhysChem*, 2009, **10**, 1084–1089.
59 T. Shimada, K. Aoki, Y. Shinoda, T. Nakamura, N. Tokunaga, S. Inagaki and T. Hayashi, *J. Am. Chem. Soc.*, 2003, **125**, 4688–4689.
60 Y. R. Yeon, Y. J. Park, J. S. Lee, J. W. Park, S. G. Kang and C. H. Jun, *Angew. Chem., Int. Ed.*, 2008, **47**, 109–112.
61 (*a*) H. Yoshitake, E. Koiso, H. Horie and H. Yoshimura, *Microporous Mesoporous Mater.*, 2005, **85**, 183–194; (*b*) A. Taguchi and F. Schüth, *Microporous Mesoporous Mater.*, 2005, **77**, 1–45; (*c*) M. H. Lim and A. Stein, *Chem. Mater.*, 1999, **11**, 3285–3295.
62 W. M. Van Rhijn, D. E. De Vos, B. F. Sels and W. D. Bossaert, *Chem. Commun.*, 1998, 317–318.
63 J. D. Bass and A. Katz, *Chem. Mater.*, 2006, **18**, 1611–1620.
64 S. J. Tavener, J. H. Clark, G. W. Gray, P. A. Heath and D. J. Macquarrie, *Chem. Commun.*, 1997, 1147–1148.
65 (*a*) D. J. Macquarrie, *Chem. Commun.*, 1996, 1961–1962; (*b*) S. L. Burkett, S. D. Sims and S. Mann, *Chem. Commun.*, 1996, 1367–1368.
66 D. J. Macquarrie, D. B. Jackson, J. E. G. Mdoe and J. H. Clark, *New J. Chem.*, 1999, **23**, 539–544.
67 I. Díaz, *J. Catal.*, 2000, **193**, 283–294.
68 (*a*) M. H. Lim, C. F. Blanford and A. Stein, *Chem. Mater.*, 1998, **10**, 467–470; (*b*) Q. Yang, M. P. Kapoor and S. Inagaki, *J. Am. Chem. Soc.*, 2002, **124**, 9694–9695.
69 D. Margolese, J. A. Melero, S. C. Christiansen, B. F. Chmelka and G. D. Stucky, *Chem. Mater.*, 2000, **12**, 2448–2459.
70 J. G. C. Shen, R. G. Herman and K. Klier, *J. Phys. Chem. B*, 2002, **106**, 9975–9978.
71 K. J. Shea, J. Moreau, D. A. Loy, R. J. P. Corriu and B. Boury, in *Functional Hybrid Materials*, eds. P. Gòmez Romero and C. Sanchez, Wiley-VCH Verlag GmbH, Weinheim, 1st edn, 2004, ch. 3, pp. 50–85.
72 S. Inagaki, S. Guan, Y. Fukushima, T. Ohsuna and O. Terasaki, *J. Am. Chem. Soc.*, 1999, **121**, 9611–9614.
73 T. Asefa, M. J. MacLachlan, N. Coombs and G. A. Ozin, *Nature*, 1999, **402**, 867–871.
74 M. Ohashi, M. P. Kapoor and S. Inagaki, *Chem. Commun.*, 2008, 841–843.
75 B. J. Melde, B. T. Holland, C. F. Blanford and A. Stein, *Chem. Mater.*, 1999, **11**, 3302–3308.
76 (*a*) C. Yoshina-Ishii, T. Asefa, N. Coombs, M. J. MacLachlan and G. A. Ozin, *Chem. Commun.*, 1999,

2539–2540; (*b*) S. Inagaki, S. Guan, T. Ohsuna and O. Terasaki, *Nature*, 2002, **416**, 304–307.
77 T. Asefa, M. Kruk, M. J. MacLachlan, N. Coombs, H. Grondey, M. Jaroniec and G. A. Ozin, *J. Am. Chem. Soc.*, 2001, **123**, 8520–8530.
78 (*a*) A. Sayari and Y. Yang, *Chem. Commun.*, 2002, 2582–2583; (*b*) S. Hamoudi and S. Kaliaguine, *Chem. Commun.*, 2002, 2118–2119.
79 T. Asefa, M. J. MacLachlan, N. Coombs and G. A. Ozin, *Nature*, 1999, **402**, 867–871.
80 (*a*) D.-J. Kim, J.-S. Chung, W.-S. Ahn, G.-W. Kang and W.-J. Cheong, *Chem. Lett.*, 2004, **33**, 422–423; (*b*) S.-S. Yoon, W.-J. Son, K. Biswas and W.-S. Ahn, *Bull. Korean Chem. Soc.*, 2008, **29**, 609–614; (*c*) B. E. Grabicka and M. Jaroniec, *Microporous Mesoporous Mater.*, 2009, **119**, 144–149.
81 D. Dubé, M. Rat, F. Béland and S. Kaliaguine, *Microporous Mesoporous Mater.*, 2008, **111**, 596–603.
82 (*a*) R. Voss, A. Thomas, M. Antonietti and G. A. Ozin, *J. Mater. Chem.*, 2005, **15**, 4010–4014; (*b*) A. Ide, R. Voss, G. Scholz, G. A. Ozin, M. Antonietti and A. Thomas, *Chem. Mater.*, 2007, **19**, 2649–2657.
83 S. Polarz and A. Kuschel, *Adv. Mater.*, 2006, **18**, 1206–1209.
84 T. Asefa, M. Kruk, M. J. MacLachlan, N. Coombs, H. Grondey, M. Jaroniec and G. A. Ozin, *Adv. Funct. Mater.*, 2001, **11**, 447–456.
85 K. Nakajima, I. Tomita, M. Hara, S. Hayashi, K. Domen and J. N. Kondo, *Adv. Mater.*, 2005, **17**, 1839–1842.
86 M. C. Burleigh, M. A. Markowitz, M. S. Spector and B. P. Gaber, *J. Phys. Chem. B*, 2001, **105**, 9935–9942.
87 (*a*) Q. Yang, J. Liu, J. Yang, M. Kapoor, S. Inagaki and C. Li, *J. Catal.*, 2004, **228**, 265–272; (*b*) P. L. Dhepe, M. Ohashi, S. Inagaki, M. Ichikawa and A. Fukuoka, *Catal. Lett.*, 2005, **102**, 163–169; (*c*) Q. Yang, M. P. Kapoor, S. Inagaki, N. Shirokura, J. N. Kondo and K. Domen, *J. Mol. Catal. A: Chem.*, 2005, **230**, 85–89; (*d*) M. Rat, M. H. Zahedi-Niaki, S. Kaliaguine and T. O. Do, *Microporous Mesoporous Mater.*, 2008, **112**, 26–31.
88 (*a*) S. Huh, J. W. Wiench, B. G. Trewyn, S. Song, M. Pruski and V. S. Y. Lin, *Chem. Commun.*, 2003, 2364–2365; (*b*) O. Olkhovyk, S. Pikus and M. Jaroniec, *J. Mater. Chem.*, 2005, **15**, 1517–1519; (*c*) W. J. Hunks and G. A. Ozin, *Adv. Funct. Mater.*, 2005, **15**, 259–266; (*d*) M. A. Wahab, I. Imae, Y. Kawakami and C.-S. Ha, *Chem. Mater.*, 2005, **17**, 2165–2174; (*e*) O. Olkhovyk and M. Jaroniec, *Ind. Eng. Chem. Res.*, 2007, **46**, 1745–1751.
89 (*a*) Y. Izumi, R. Hasebe and K. Urabe, *J. Catal.*, 1983, **84**, 402–409; (*b*) C. Rocchiccioli-Deltcheff, M. Amirouche, G. Herve, M. Fournier, M. Che and J. M. Tatibouet, *J. Catal.*, 1990, **126**, 591–599.
90 Y. Ren, B. Yue, M. Gu and H. He, *Materials*, 2010, **3**, 764–785.
91 J. Helminen and E. Paatero, *React. Funct. Polym.*, 2006, **66**, 1021–1032.
92 E. Carlier, A. Guyot, A. Revillon, M.-F. Llauro-Darricades and R. Petiaud, *React. Polym.*, 1991, **16**, 41–49.
93 M. Fujiwara, F. Yamamoto, K. Okamoto, K. Shiokawa and R. Nomura, *Anal. Chem.*, 2005, **77**, 8138–8145.
94 M. A. Harmer, Q. Sun, A. J. Vega, W. E. Farneth, A. Heidekum and W. F. Hoelderich, *Green Chem.*, 2000, **2**, 7–14.
95 C. G. Wu and T. Bein, *Science*, 1994, **264**, 1757–1759.
96 S. A. Johnson, D. Khushalani, N. Coombs, T. E. Mallouk and G. A. Ozin, *J. Mater. Chem.*, 1998, **8**, 13–14.
97 P. L. Llewellyn, U. Ciesla, H. Decher, R. Stadler, F. Schüth and K. K. Unger, *Stud. Surf. Sci. Catal.*, 1994, **84**, 2013–2020.
98 C. G. Wu and T. Bein, *Science*, 1994, **266**, 1013–1015.
99 K. Kageyama, *Science*, 1999, **285**, 2113–2115.
100 (*a*) M. T. Run, S. Z. Wu, D. Y. Zhang and G. Wu, *Mater. Chem. Phys.*, 2007, **105**, 341–347; (*b*) S. Mien, S.-i. Ogino, T. Aida, K. A. Koyano and T. Tatsumi, *Macromol. Rapid Commun.*, 1997, **18**, 991–996.
101 R. J. Kalbasi, M. Kolahdoozan and M. Rezaei, *Mater. Chem. Phys.*, 2011, **125**, 784–790.
102 (*a*) F. de Clippel, A. Harkiolakis, X. Ke, T. Vosch, G. Van Tendeloo, G. V. Baron, P. A. Jacobs, J. F. Denayer and B. F. Sels, *Chem. Commun.*, 2010, **46**, 928–930; (*b*) F. de Clippel, A. Harkiolakis, T. Vosch, X. Ke, L. Giebeler, S. Oswald, K. Houthoofd, J. Jammaer, G. Van Tendeloo, J. A. Martens, P. A. Jacobs, G. V. Baron, B. F. Sels and J. F. M. Denayer, *Microporous Mesoporous Mater.*, 2011, **144**, 120–133.
103 S. Spange, B. Heublein, A. Schramm and R. Martinez, *Macromol. Rapid Commun.*, 2003, **13**, 511–515.
104 (*a*) R. J. Kalbasi and E. Izadi, *C. R. Chim.*, 2011, **14**, 1002–1013; (*b*) R. J. Kalbasi, M. Kolahdoozan and S. M. Vanani, *J. Solid State Chem.*, 2011, **184**, 2009–2016.
105 (*a*) M. Fujiwara, K. Kuraoka, T. Yazawa, Q. Xu, M. Tanaka and Y. Souma, *Chem. Commun.*, 2000, 1523–1524; (*b*) Y. S. Kang, H. I. Lee, Y. Zhang, Y. J. Han, J. E. Yie, G. D. Stucky and J. M. Kim, *Chem. Commun.*, 2004, 1524–1525; (*c*) M. Fujiwara, K. Shiokawa and Y. Zhu, *J. Mol. Catal. A: Chem.*, 2007, **264**, 153–161.
106 M. A. Harmer, W. E. Farneth and Q. Sun, *J. Am. Chem. Soc.*, 1996, **118**, 7708–7715.
107 (*a*) J. Surowiec and R. Bogoczek, *J. Therm. Anal. Calorim.*, 1988, **33**, 1097–1102; (*b*) C. A. Wilkie, J. R. Thomsen and M. L. Mittleman, *J. Appl. Polym. Sci.*, 1991, **42**, 901–909.
108 (*a*) J. H. Knox and B. Kaur, *J. Chromatogr., A*, 1986, **352**, 3–25; (*b*) J. Lee, S. Yoon, S. M. Oh, C.-H. Shin and T. Hyeon, *Adv. Mater.*, 2000, **12**, 359–362; (*c*) J. Lee, S. Yoon, T. Hyeon, S. M. Oh and K. B. Kimb, *Chem. Commun.*, 1999, 2177–2178.
109 A. M. B. Furtado, Y. Wang and M. D. LeVan, *Microporous Mesoporous Mater.*, 2013, **165**, 48–54.
110 F. de Clippel, M. Dusselier, R. Van Rompaey, P. Vanelderen, J. Dijkmans, E. Makshina, L. Giebeler, S. Oswald, G. V. Baron, J. F. Denayer, P. P. Pescarmona, P. A. Jacobs and B. F. Sels, *J. Am. Chem. Soc.*, 2012, **134**, 10089–10101.

111 T. G. Glover, K. I. Dunne, R. J. Davis and M. D. LeVan, *Microporous Mesoporous Mater.*, 2008, **111**, 1–11.
112 R. J. White, V. Budarin, R. Luque, J. H. Clark and D. J. Macquarrie, *Chem. Soc. Rev.*, 2009, **38**, 3401–3418.
113 R. J. White, V. L. Budarin and J. H. Clark, *ChemSusChem*, 2008, **1**, 408–411.
114 C. L. Burket, R. Rajagopalan, A. P. Marencic, K. Dronvajjala and H. C. Foley, *Carbon*, 2006, **44**, 2957–2963.
115 R. Ryoo, S. H. Joo and S. Jun, *J. Phys. Chem. B*, 1999, **103**, 7743–7746.
116 M.-M. Titirici, M. Antonietti and N. Baccile, *Green Chem.*, 2008, **10**, 1204–1212.
117 Q. Yue, M. Wang, J. Wei, Y. Deng, T. Liu, R. Che, B. Tu and D. Zhao, *Angew. Chem., Int. Ed.*, 2012, **124**, 1–6.
118 S.-S. Kim, D.-K. Lee, J. Shah and T. J. Pinnavaia, *Chem. Commun.*, 2003, 1436–1437.
119 R. K. Mariwala and H. C. Foley, *Ind. Eng. Chem. Res.*, 1994, **33**, 607–615.
120 (*a*) D. S. Lafyatis, J. Tung and H. C. Foley, *Ind. Eng. Chem. Res.*, 1991, **30**, 865–873; (*b*) D. S. Lafyatis, R. K. Mariwala, E. E. Lowenthal and H. C. Foley, *Design and Synthesis of Carbon Molecular Sieves for Separation and Catalysis*, Van Nostrand, New York, 1992.
121 P. Vinke, M. Van Der Elik, M. Verbree, A. F. Voskamp and H. Van Bekkum, *Carbon*, 1994, **32**, 675–686.
122 G. Chen and B. Fang, *Bioresour. Technol.*, 2011, **102**, 2635–2640.
123 (*a*) M. Hara, T. Yoshida, A. Takagaki, T. Takata, J. N. Kondo, S. Hayashi and K. Domen, *Angew. Chem., Int. Ed.*, 2004, **43**, 2955–2958; (*b*) M. Toda, A. Takagaki, M. Okamura, J. N. Kondo, S. Hayashi, K. Domen and M. Hara, *Nature*, 2005, **438**, 178; (*c*) M. Okamura, A. Takagaki, M. Toda, J. N. Kondo, K. Domen, T. Tatsumi, M. Hara and S. Hayashi, *Chem. Mater.*, 2006, **18**, 3039–3045; (*d*) V. Budarin, J. H. Clark, J. J. Hardy, R. Luque, K. Milkowski, S. J. Tavener and A. J. Wilson, *Angew. Chem., Int. Ed.*, 2006, **45**, 3782–3786.
124 L. Fang, K. Zhang, X. Li, H. Wu and P. Wu, *Chin. J. Catal.*, 2012, **33**, 114–122.
125 A. L. W. Demuynck, L. Peng, F. de Clippel, J. Vanderleyden, P. A. Jacobs and B. F. Sels, *Adv. Synth. Catal.*, 2011, **353**, 725–732.
126 S. Van de Vyver, L. Peng, J. Geboers, H. Schepers, F. de Clippel, C. J. Gommes, B. Goderis, P. A. Jacobs and B. F. Sels, *Green Chem.*, 2010, **12**, 1560–1563.
127 M. S. Shafeeyan, W. M. A. W. Daud, A. Houshmand and A. Shamiri, *J. Anal. Appl. Pyrolysis*, 2010, **89**, 143–151.
128 (*a*) J. Lahaye, G. Nanse, A. Bagreev and V. Strelko, *Carbon*, 1999, **37**, 585–590; (*b*) A. Lu, A. Kiefer, W. Schmidt and F. Schüth, *Chem. Mater.*, 2004, **16**, 100–103; (*c*) C.-M. Yang, C. Weidenthaler, B. Spliethoff, M. Mayanna and F. Schüth, *Chem. Mater.*, 2005, **17**, 355–358; (*d*) M. Lezanska, J. Wloch and J. Kornatowski, *Stud. Surf. Sci. Catal.*, 2008, **174B**, 945–948.
129 R. M. Freire, A. H. Morais Batista, A. G. Souza Filho, J. M. Filho, G. D. Saraiva and A. C. Oliveira, *Catal. Lett.*, 2009, **131**, 135–145.
130 Y. Liu, J. Chen, J. Yao, Y. Lu, L. Zhang and X. Liu, *Chem. Eng. J.*, 2009, **148**, 201–206.
131 K. Nakajima, M. Okamura, J. N. Kondo, K. Domen, T. Tatsumi, S. Hayashi and M. Hara, *Chem. Mater.*, 2009, **21**, 186–193.
132 M. Ogura, Y. Zhang, S. P. Elangovan and T. Okubo, *Microporous Mesoporous Mater.*, 2007, **101**, 224–230.
133 J. S. Lee, X. Wang, H. Luo, G. A. Baker and S. Dai, *J. Am. Chem. Soc.*, 2009, **131**, 4596–4597.
134 (*a*) L. Zhi, J. Wang, G. Cui, M. Kastler, B. Schmaltz, U. Kolb, U. Jonas and K. Müllen, *Adv. Mater.*, 2007, **19**, 1849–1853; (*b*) L. Zhi, Y.-S. Hu, B. E. Hamaoui, X. Wang, I. Lieberwirth, U. Kolb, J. Maier and K. Müllen, *Adv. Mater.*, 2008, **20**, 1727–1731.
135 T. J. Wooster, K. M. Johanson, K. J. Fraser, D. R. MacFarlane and J. L. Scott, *Green Chem.*, 2006, **8**, 691.
136 (*a*) J. S. Lee, X. Wang, H. Luo and S. Dai, *Adv. Mater.*, 2010, **22**, 1004–1007; (*b*) J. P. Paraknowitsch, J. Zhang, D. Su, A. Thomas and M. Antonietti, *Adv. Mater.*, 2010, **22**, 87–92.
137 X. Wang and S. Dai, *Angew. Chem., Int. Ed.*, 2010, **49**, 6664–6668.
138 S. Zhu, H. Zhou, M. Hibino, I. Honma and M. Ichihara, *Mater. Chem. Phys.*, 2004, **88**, 202–206.
139 M. M. L. Ribeiro Carrott, A. J. Estevao Candeias, P. J. M. Carrott, K. S. W. Sing and K. K. Unger, *Langmuir*, 2000, **16**, 9103–9105.
140 H. Nishihara, Y. Fukura, K. Inde, K. Tsuji, M. Takeuchi and T. Kyotani, *Carbon*, 2008, **46**, 48–53.
141 L. Chuenchom, R. Kraehnert and B. M. Smarsly, *Soft Matter*, 2012, **8**, 10801.
142 C. Liang, K. Hong, G. A. Guiochon, J. W. Mays and S. Dai, *Angew. Chem., Int. Ed.*, 2004, **43**, 5785–5789.
143 Y. Deng, T. Yu, Y. Wan, Y. Shi, Y. Meng, D. Gu, L. Zhang, Y. Huang, C. Liu, X. Wu and D. Zhao, *J. Am. Chem. Soc.*, 2007, **129**, 1690–1697.
144 (*a*) C. Liu, L. Li, H. Song and X. Chen, *Chem. Commun.*, 2007, 757–759; (*b*) F. Zhang, Y. Meng, D. Gu, Y. Yan, C. Yu, B. Tu and D. Zhao, *J. Am. Chem. Soc.*, 2005, **127**, 13508–13509; (*c*) C. Liang and S. Dai, *J. Am. Chem. Soc.*, 2006, **128**, 5316–5317; (*d*) S. Tanaka, N. Nishiyama, Y. Egashira and K. Ueyama, *Chem. Commun.*, 2005, 2125–2127.
145 Y. Meng, D. Gu, F. Zhang, Y. Shi, H. Yang, Z. Li, C. Yu, B. Tu and D. Zhao, *Angew. Chem., Int. Ed.*, 2005, **44**, 7053–7059.
146 X. Wang, C. Liang and S. Dai, *Langmuir*, 2008, **24**, 7500–7505.
147 Y. Meng, D. Gu, F. Zhang, Y. Shi, L. Cheng, D. Feng, Z. Wu, Z. Chen, Y. Wan, A. Stein and D. Zhao, *Chem. Mater.*, 2006, 18.
148 X. Qian, H. Li and Y. Wan, *Microporous Mesoporous Mater.*, 2011, **141**, 26–37.

149 D. Long, W. Qiao, L. Zhan, X. Liang and L. Ling, *Microporous Mesoporous Mater.*, 2009, **121**, 58–66.
150 S. Tanaka, A. Doi, N. Nakatani, Y. Katayama and Y. Miyake, *Carbon*, 2009, **47**, 2688–2698.
151 Y. Deng, J. Liu, C. Liu, D. Gu, Z. Sun, J. Wei, J. Zhang, L. Zhang, B. Tu and D. Zhao, *Chem. Mater.*, 2008, **20**, 7281–7286.
152 Y. Deng, Y. Cai, Z. Sun, D. Gu, J. Wei, W. Li, X. Guo, J. Yang and D. Zhao, *Adv. Funct. Mater.*, 2010, **20**, 3658–3665.
153 H.-P. Lin, C.-Y. Chang-Chien, C.-Y. Tang and C.-Y. Lin, *Microporous Mesoporous Mater.*, 2006, **93**, 344–348.
154 R. Liu, Y. Shi, Y. Wan, Y. Meng, F. Zhang, D. Gu, Z. Chen, B. Tu and D. Zhao, *J. Am. Chem. Soc.*, 2006, **128**, 11652–11662.
155 C. J. Brinker, Y. Lu, A. Sellinger and H. Fan, *Adv. Mater.*, 1999, **11**, 579–585.
156 Q. Hu, R. Kou, J. Pang, T. L. Ward, M. Cai, Z. Yang, Y. Lu and J. Tang, *Chem. Commun.*, 2007, 601–603.
157 J. Liu, S. Z. Qiao, H. Liu, J. Chen, A. Orpe, D. Zhao and G. Q. Lu, *Angew. Chem., Int. Ed.*, 2011, **50**, 5947–5951.
158 X. Zhang, Y. Li and C. Cao, *J. Mater. Chem.*, 2012, **22**, 13918–13921.
159 C.-J. Li, *Chem. Rev.*, 2005, **105**, 3095–3165.
160 Y. Chen, Z. Guo, T. Chen and Y. Yang, *J. Catal.*, 2010, **275**, 11–24.
161 (*a*) E. Sujandi, E. A. Prasetyanto and S.-E. Park, *Appl. Catal., A*, 2008, **350**, 244–251; (*b*) S.-Y. Chen, C.-Y. Huang, T. Yokoi, C.-Y. Tang, S.-J. Huang, J.-J. Lee, J. C. C. Chan, T. Tatsumi and S. Cheng, *J. Mater. Chem.*, 2012, **22**, 2233–2243.
162 A. C. Coelho, S. S. Balula, S. M. Bruno, J. C. Alonso, N. Bion, P. Ferreira, M. Pillinger, A. A. Valente, J. Rocha and I. S. Gonçalves, *Adv. Synth. Catal.*, 2010, **352**, 1759–1769.
163 Y. Wan, H. Wang, Q. Zhao, M. Klingstedt, O. Terasaki and D. Zhao, *J. Am. Chem. Soc.*, 2009, **131**, 4541–4550.
164 W. M. Van Rhijn, D. E. De Vos, W. D. Bossaert, J. Bullen, B. Wouters, P. J. Grobet and P. A. Jacobs, *Stud. Surf. Sci. Catal.*, 1998, **117**, 183–190.
165 (*a*) D. E. De Vos, M. Dams, B. F. Sels and P. A. Jacobs, *Chem. Rev.*, 2002, **102**, 3615–3640; (*b*) A. Corma and H. García, *Chem. Rev.*, 2002, **102**, 3837–3892.
166 E. Poli, R. De Sousa, F. Jérome, Y. Pouilloux and J.-M. Clacens, *Catal. Sci. Technol.*, 2012, **2**, 910–914.
167 C. Zapilko, Y. Liang, W. Nerdal and R. Anwander, *Chem.–Eur. J.*, 2007, **13**, 3169–3176.
168 H. C. Foley, *Microporous Mater.*, 1995, **4**, 407–433.
169 D. S. Lafyatis, Ph.D., University of Delaware, 1991.
170 H. C. Foley, D. S. Lafyatis, R. K. Mariwala, G. D. Sonnichsen and L. D. Brake, *Chem. Eng. Sci.*, 1995, **49**, 4771–4786.
171 F. de Clippel, A. L. Khan, A. Cano-Odena, M. Dusselier, K. Vanherck, L. Peng, S. Oswald, L. Giebeler, S. Corthals, B. Kenens, J. F. M. Denayer, P. A. Jacobs, I. F. J. Vankelecom and B. F. Sels, *J. Mater. Chem. A*, 2013, **1**, 945.
172 T. Zheng, Y.-R. Dong, N. Nishiyama, Y. Egashira and K. Ueyama, *Appl. Catal., A*, 2006, **308**, 210–215.
173 Q. Sun, A. Harmer and W. E. Farneth, *Chem. Commun.*, 1996, 1201–1203.
174 Q. Sun, M. A. Harmer and W. E. Farneth, *Ind. Eng. Chem. Res.*, 1997, **36**, 5541–5544.
175 (*a*) Q. Sun, W. E. Farneth and M. A. Harmer, *J. Catal.*, 1996, **164**, 62–69; (*b*) A. Heidekum, M. A. Harmer and W. F. Hölderich, *Catal. Lett.*, 1997, **47**, 243–246.
176 (*a*) A. Heidekum, M. A. Harmer and W. F. Hoelderich, *J. Catal.*, 1996, **176**, 260–263; (*b*) A. Heidekum, A. Harmer and W. F. Hoelderich, *J. Catal.*, 1999, **181**, 217–222; (*c*) A. Heidekum, A. Harmer and W. F. Hoelderich, *J. Catal.*, 1999, **188**, 230–232.
177 (*a*) L. T. Zhuralev, *Colloids Surf., A*, 1993, **74**, 71–90; (*b*) A. Cauvel, D. Brunel and F. Di Renzo, *Langmuir*, 1997, **13**, 2773–2778.
178 B. Sels, E. D'Hondt and P. Jacobs, in *Catalysis for Renewables: From Feedstock to Energy Production*, eds. G. Centi and R. A. van Santen, Wiley-VCH Verlag GmbH & Co. KGaA, Weinheim, 2007, ch. 11.
179 (*a*) E. D'Hondt, S. Van de Vyver, B. F. Sels and P. A. Jacobs, *Chem. Commun.*, 2008, 6011–6012; (*b*) L. Li, T. I. Korányi, B. F. Sels and P. P. Pescarmona, *Green Chem.*, 2012, **14**, 1611; (*c*) P. P. Pescarmona, K. P. F. Janssen, C. Delaet, C. Stroobants, K. Houthoofd, A. Philippaerts, C. De Jonghe, J. S. Paul, P. A. Jacobs and B. F. Sels, *Green Chem.*, 2010, **12**, 1083.
180 A. Karam, Y. Gu, F. Jerome, J. P. Douliez and J. Barrault, *Chem. Commun.*, 2007, 2222–2224.
181 I. Dıaz, F. Mohino, J. Pérez-Pariente and E. Sastre, *Appl. Catal., A*, 2001, **205**, 19–30.
182 Y. Gu, A. Azzouzi, Y. Pouilloux, F. Jérôme and J. Barrault, *Green Chem.*, 2008, **10**, 164–167.
183 J. A. Melero, G. Vicente, G. Morales, M. Paniagua, J. M. Moreno, R. Roldán, A. Ezquerro and C. Pérez, *Appl. Catal., A*, 2008, **346**, 44–51.
184 G. Kharchafi, F. Jérôme, I. Adam, Y. Pouilloux and J. Barrault, *New J. Chem.*, 2005, **29**, 928–934.
185 I. Díaz, *J. Catal.*, 2000, **193**, 295–302.
186 (*a*) Y. Gu, C. Ogawa, J. Kobayashi, Y. Mori and S. Kobayashi, *Angew. Chem., Int. Ed.*, 2006, **45**, 7217–7220; (*b*) Y. Gu, A. Karam, F. Jérôme and J. Barrault, *Org. Lett.*, 2007, **9**, 3145–3148.
187 B. Sow, S. Hamoudi, M. Hassan Zahedi-Niaki and S. Kaliaguine, *Microporous Mesoporous Mater.*, 2005, **79**, 129–136.
188 A. Karam, J. C. Alonso, T. I. Gerganova, P. Ferreira, N. Bion, J. Barrault and F. Jerome, *Chem. Commun.*, 2009, 7000–7002.
189 (*a*) M. Alvaro, A. Corma, D. Das, V. Fornes and H. Garcia, *Chem. Commun.*, 2004, 956–957; (*b*) M. Alvaro, A. Corma, D. Das, V. Fornes and H. Garcia, *J. Catal.*, 2005, **231**, 48–55.
190 G. Grigoropoulou, J. H. Clark and J. A. Elings, *Green Chem.*, 2003, **5**, 1–7.

191 (*a*) T. Blasco, A. Corma, M. T. Navarro and J. N. Pérez-Pariente, *J. Catal.*, 1995, **156**, 65–74; (*b*) A. Corma, P. Esteve and A. Martínez, *J. Catal.*, 1996, **161**, 11–19.
192 I. Diaz and J. Pérez-Pariente, *Chem. Mater.*, 2002, **14**, 4641–4646.
193 S. Van de Vyver, J. Geboers, P. A. Jacobs and B. F. Sels, *ChemCatChem*, 2011, **3**, 82–94.
194 M. Dusselier, P. Van Woγuwe, A. Dewaele, E. Makshina and B. F. Sels, *Energy Environ. Sci.*, 2013, **6**, 1415–1442.
195 M. Dusselier, P. V. Wouwe, F. d. Clippel, J. Dijkmans, D. W. Gammon and B. F. Sels, *ChemCatChem*, 2013, **5**, 569–575.
196 J. Alauzun, A. Mehdi, C. Reye and R. J. P. Corriu, *J. Am. Chem. Soc.*, 2006, **128**, 8718–8719.
197 S. Shylesh, A. Wagener, A. Seifert, S. Ernst and W. R. Thiel, *Angew. Chem., Int. Ed.*, 2010, **49**, 184–187.
198 D. Srinivas and P. Ratnasamy, *Microporous Mesoporous Mater.*, 2007, **105**, 170–180.
199 V. Dufaud and M. E. Davis, *J. Am. Chem. Soc.*, 2003, **125**, 9403–9413.
200 D. Coutinho, S. Madhugiri and K. J. Balkus Jr., *J. Porous Mater.*, 2004, **11**, 239–254.
201 (*a*) R. K. Zeidan, S. J. Hwang and M. E. Davis, *Angew. Chem., Int. Ed.*, 2006, **45**, 6332–6335; (*b*) R. K. Zeidan and M. E. Davis, *J. Catal.*, 2007, **247**, 379–382.
202 Y. Kubota, K. Goto, S. Miyata, Y. Goto, Y. Fukushima and Y. Sugi, *Chem. Lett.*, 2003, **32**, 234–235.
203 N. A. Brunelli, K. Venkatasubbaiah and C. W. Jones, *Chem. Mater.*, 2012, **24**, 2433–2442.
204 (*a*) Y. Kubota, H. Yamaguchi, T. Yamada, S. Inagaki, Y. Sugi and T. Tatsumi, *Top. Catal.*, 2010, **53**, 492–499; (*b*) Y. Xie, K. K. Sharma, A. Anan, G. Wang, A. V. Biradar and T. Asefa, *J. Catal.*, 2009, **265**, 131–140.
205 (*a*) K. K. Sharma and T. Asefa, *Angew. Chem., Int. Ed.*, 2007, **46**, 2879–2882; (*b*) J. D. Bass, A. Solovyov, A. J. Pascall and A. Katz, *J. Am. Chem. Soc.*, 2006, **128**, 3737–3747.
206 N. A. Brunelli, S. A. Didas, K. Venkatasubbaiah and C. W. Jones, *J. Am. Chem. Soc.*, 2012, **134**, 13950–13953.
207 (*a*) S. Van de Vyver, S. Helsen, J. Geboers, F. Yu, J. Thomas, M. Smet, W. Dehaen, Y. Román-Leshkov, I. Hermans and B. F. Sels, *ACS Catal.*, 2012, **2**, 2700–2704; (*b*) S. Van de Vyver, J. Geboers, S. Helsen, F. Yu, J. Thomas, M. Smet, W. Dehaen and B. F. Sels, *Chem. Commun.*, 2012, **48**, 3497–3499.
208 E. L. Margelefsky, R. K. Zeidan and M. E. Davis, *Chem. Soc. Rev.*, 2008, **37**, 1118–1126.
209 E. L. Margelefsky, R. K. Zeidan, V. Dufaud and M. E. Davis, *J. Am. Chem. Soc.*, 2007, **129**, 13691–13697.
210 L. Jiao and J. R. Regalbuto, *J. Catal.*, 2008, **260**, 342–350.
211 M. Arai, S.-L. Guo and Y. Nishiyama, *Appl. Catal.*, 1991, **77**, 141–148.
212 F. Su, L. Lv, F. Y. Lee, T. Liu, A. I. Cooper and X. S. Zhao, *J. Am. Chem. Soc.*, 2007, **129**, 14213–14223.
213 W. Chen, X. Pan, M.-G. Willinger, D. S. Su and X. Bao, *J. Am. Chem. Soc.*, 2006, **128**, 3136–3137.
214 A.-H. Lu, J.-J. Nitz, M. Comotti, C. Weidenthaler, K. Schlichte, C. W. Lehmann, O. Terasaki and F. Schüth, *J. Am. Chem. Soc.*, 2010, **132**, 14152–14162.
215 (*a*) I. F. J. Vankelecom and P. A. Jacobs, in *Chiral Catalyst Immobilization and Recycling*, ed. D. E. De Vos, I. F. J. Vankelecom and P. A. Jacobs, Wiley-VCH Verlag GmbH, Weinheim, 2000, ch. 2, pp. 19–42; (*b*) P. McMorn and G. J. Hutchings, *Chem. Soc. Rev.*, 2004, **33**, 108–122; (*c*) B. M. L. Dioos, I. F. J. Vankelecom and P. A. Jacobs, *Adv. Synth. Catal.*, 2006, **348**, 1413–1446.
216 K. Cassiers, T. Linssen, M. Mathieu, M. Benjelloun, K. Schrijnemakers, P. V. D. Voort, P. Cool and E. F. Vansant, *Chem. Mater.*, 2002, **14**, 2317–2324.
217 X. S. Zhao, G. Q. Lu and X. Hu, *Microporous Mesoporous Mater.*, 2000, **41**, 37–47.
218 S. S. Kim, W. Zhang and T. J. Pinnavaia, *Science*, 1998, **282**, 1302–1305.
219 (*a*) J. M. Kisler, M. L. Gee, G. W. Stevens and A. J. O'Connor, *Chem. Mater.*, 2003, **15**, 619–624; (*b*) M. Kruk, E. B. Celer and M. Jaroniec, *Chem. Mater.*, 2004, **16**, 698–707.
220 T. Tatsumi, K. A. Koyano, Y. Tanaka and S. Nakata, *Chem. Lett.*, 1997, 469–470.
221 A. C. Coelho, S. S. Balula, M. M. Antunes, T. I. Gerganova, N. Bion, P. Ferreira, M. Pillinger, A. A. Valente, J. Rocha and I. S. Gonçalves, *J. Mol. Catal. A: Chem.*, 2010, **332**, 13–18.
222 D. J. Macquarrie, S. J. Tavener and M. A. Harmer, *Chem. Commun.*, 2005, 2363–2365.
223 R. Ciriminna, J. Blum, D. Avnir and M. Pagliaro, *Chem. Commun.*, 2000, 1441–1442.

